Università degli Studi di Padova
Dipartimento di Biologia
Corso di Laurea Magistrale in Marine Biology

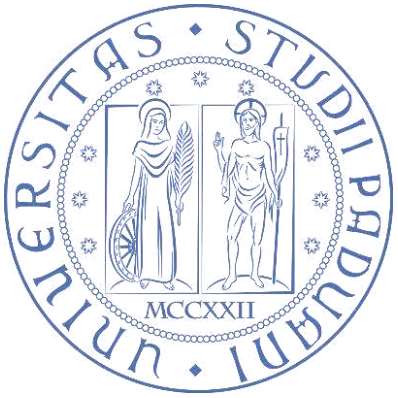

Tesi di Laurea

Benthic habitat mapping and classification from acoustic and ROV data processing - Pontine Islands case study

Relatore: Dott.ssa Laura Airoldi
Dipartamento di Biologia

Correlatore: Federica Foglini
CNR ISMAR

Laureando: Ábel Fülep

Anno Accademico 2023/2024

Table of contents

Abstract

Accurate and comprehensive mapping of marine environments is crucial for understanding ecological dynamics, biodiversity distribution and facilitating effective conservation strategies (Hughes et al., 2021). This study presents a comprehensive approach to benthic habitat mapping and classification, leveraging the integration of acoustic data and ROV observations. It contributes to data acquisition at a specific area, located at the Pontine Islands in the Tyrrhenian Sea. Adds to the ongoing worldwide mapping efforts, with the goal of obtaining detailed information on the substrate types and benthic habitats. It focuses also on the identification of possible rhodolith beds, present in the area, through the characterization of the seafloor and by analyzing ground truthing samples.

Detailed morphological information, high-quality terrain attributes, data on substrate types and habitat extensions were obtained. A high-resolution substrate map was derived, showing the extension of 5 different substrate types, classified by CoDeMap scheme, with a predictive accuracy of 59.58%. During the analysis, 398 organisms were found and successfully identified, from 37 distinct taxa, while dense aggregations of rhodoliths, were present in 67.95% of the samples. Validated benthic habitat maps were constructed with estimated locations and extensions of rhodolith beds, adding to the available datasets, helping to build more reliable, large-scale species distribution and habitat maps as well. Knowing the locations of these vulnerable habitats and determining their current state is important, both for monitoring and preserving the marine ecosystems. Enhancing the precision and reliability of new findings can contribute greatly to national conservation and effective management strategies.

1. Introduction

The world's oceans and seas are home to a diverse array of ecosystems that play a crucial role in maintaining the Earth's biodiversity and regulating global climate systems. Among these ecosystems, benthic habitats, which include the seabed and its associated flora and fauna, serve as critical components of marine environments. Understanding and characterizing these habitats is essential for the conservation of marine biodiversity, fisheries management, and the sustainable use of ocean resources (Costello et al., 2010).

Accurate mapping and classification of benthic habitats have long been a challenging task, due to the inaccessibility of the seafloor and the vastness of the world's oceans. However, recent advancements in underwater technology, such as application of rapidly progressing acoustic survey techniques (Lurton, 2002), or the deployment of Remotely Operated Vehicles (ROVs), have revolutionized our ability to explore and document these habitats (Levin et al., 2012). Acoustic methods, including multibeam and side-scan sonar, provide high-resolution images of the seafloor, allowing researchers to detect benthic features (Brown et al., 2009) and to create detailed bathymetric maps. While ROVs equipped with modern cameras and sensors enable direct observation and sampling of benthic communities at depths that were once inaccessible (Watling et al., 2013). The accuracy of predicting seabed sediments and benthic biodiversity distributions, using the combination of acoustic remote sensing and ROV observations, becomes higher and more consistent. Therefore, this type of supervised classification has gained the consensus of many experts and scholars (Lucieer et al., 2013).

This study presents a comprehensive approach to benthic habitat mapping and classification, leveraging the integration of acoustic data and ROV observations. With the synergy of these two technologies we can enhance our understanding of benthic ecosystems and improve the accuracy of habitat classification (Lecours et al. 2015). Obtaining a growing number of detailed benthic habitat maps worldwide is crucial for marine spatial planning, which helps balance human activities, conservation, and protection of marine environments (Douvere, 2008). The case study, described in this thesis, conducted in the Tyrrhenian Sea (Italy), between Palmarola and Ponza Islands adds to the mapping efforts conducted in the area, as well as emphasizes the importance of combining multiple data sources to address complex questions in marine science.

The work was conducted in the framework of the European Union's Marine Strategy Framework Directive (MSFD), aimed at achieving and maintaining Good Environmental Status (GES) of marine waters (MSFD-2008/56/CE; Long, 2015), by serving as a potential framework for marine environmental management measures within the EU. Monitoring the benthic habitats (as an example the extension of rhodolith beds) present in the Tyrrhenian Sea helps to attain the goals

of the Directive, by providing practical information on the condition and status of these protected habitats.

1.1. Mapping Marine Environments

Accurate and comprehensive mapping of marine environments is crucial for understanding ecological dynamics, biodiversity distribution and facilitating effective conservation strategies (Hughes et al., 2021). The World ocean is covering more than seventy percent of Earth's surface and holds an estimated ninety-seven percent of all available water. A great part of the intricate ecosystems, occupying this vast environment are not yet discovered. Approximately eighty percent of the ocean was never explored, studied or mapped by humans. Even with today's most advanced technologies it is almost impossible to map the entire water body and seafloor. Regardless, progressively more and more information has been collected and studied to better understand the global state of these environments.

Satellite technologies can offer a proper solution to the difficulties of mapping at such extent. NASA's Earth Observing System and the European Space Agency's Sentinel satellites, have revolutionized marine mapping. Using remote sensing methods can provide high-resolution data, enabling scientist to observe parameters like sea surface temperature, chlorophyll concentration and depth at a global scale. As a consequence of the distance between them and the observed domain, as well as sensory limitations (Al-Wassai and Kalyankar, 2013) the spectral and spatial resolutions are still not adequate enough for detailed mapping at this scale. Airborne LiDAR systems are successfully employed in nautical charting and mapping mostly at coastal environments. They are capable of recording detailed topographic information, in a relatively short time frame (Wozencraft and Millar, 2005). As the technology advances, they are going to represent a cost efficient and accurate solution to obtain large scale bathymetric maps as well. In the recent years, the deployment of Autonomous Underwater Vehicles (AUVs) equipped with advanced sonar systems and cameras allows for detailed mapping of the water column and seafloor (Winn et al., 2014), while reducing the labour intensiveness of the field. As mapping technologies advance, challenges persist. The incomplete bathymetric coverage, especially in remote areas and the need for standardized mapping protocols are ongoing concerns. Understanding the seafloor is fundamental to comprehending marine ecosystems. The General Bathymetric Chart of the Oceans (GEBCO) project stands out for its significant contribution to producing an extensive, global bathymetric map. This initiative integrates data from ship soundings, satellite imagery and airborne altimetry measurements. In addition, the Seabed 2030 project, proposed by The Nippon Foundation is aiming map the entire ocean floor by 2030 (Mayer et al. 2018).

1.1.1. Benthic habitat mapping

Benthic habitats are vital components of marine ecosystems, consisting in the ocean floor and in array of diverse organisms related with it. Mapping benthic habitat became a specialized field within marine science, focusing mostly on the spatial distribution of species and their interaction with the seafloor. It studies the factors shaping these environments, while providing techniques and implications to understand these complex systems. The early benthic habit mapping attempts associated the visible and physically obtainable substrate pieces, to the organisms found on them. Nowadays sophisticated methods are in use, combining optical and acoustic data with expert knowledge on environmental preferences and ground truthing samples, to classify parts of the seafloor with unprecedented details (Diaz et al., 2014), sometimes focusing only on the distribution of certain species.

Many strategies are currently in use to produce valuable benthic habitat maps, including: abiotic surrogate mapping, assemble first - predict later, also called unsupervised classification or predict first - assemble later, considered supervised classification (Brown et al., 2011). Moreover, the classification methods can also differ. Visual classification relies fully on expert's knowledge, thus containing larger volumes of information, but it can be subjective, time-consuming and expensive. Contrary, semi-automated or fully automated classification utilizes some kind of algorithm, which can be tuned for specific purposes. Advanced algorithms, including machine learning and AI tools, play an increasingly prominent role in processing large datasets. These technologies rely on the efficient automation of object and feature recognition. The only limitation is their accuracy or missing information about their accuracy in certain situations. There is not yet a widely accepted agreement on which is the best way from these methods.

Understanding the distribution of benthic habitats and their current state supports conservation strategies. By taking into consideration as many criteria as possible (including physical characteristics, biological diversity, functional aspects, human impacts, etc.) benthic habitat maps can help in establishment of marine protected areas worldwide.

1.2. Rhodolith beds and their importance

Rhodoliths are unattached, free-living, and calcareous coralline red algae (Rhodophyta) that form small, spherical to subspherical structures, accumulated on the seafloor **(Fig.1)**. These structures, known also as maërl, consist of multiple layers of calcium carbonate encrusted by the red algal tissue. Rhodoliths can vary in size from a few millimeters to several centimeters in diameter. The exact number of rhodolith forming species and their diversity is still a debate due to particularly difficult identification (Rösler et al., 2016) and taxonomic uncertainties (Hernández-Kantún et. al, 2017). A comprehensive study from 2021, reviewing their worldwide distribution, worked with 106 rhodolith forming species, representing 21 genera. The most abundant and diverse families being the Lithothamniaceae and Lithophyllaceae, with 26 and 28 species, respectively (Rebelo et al., 2021).

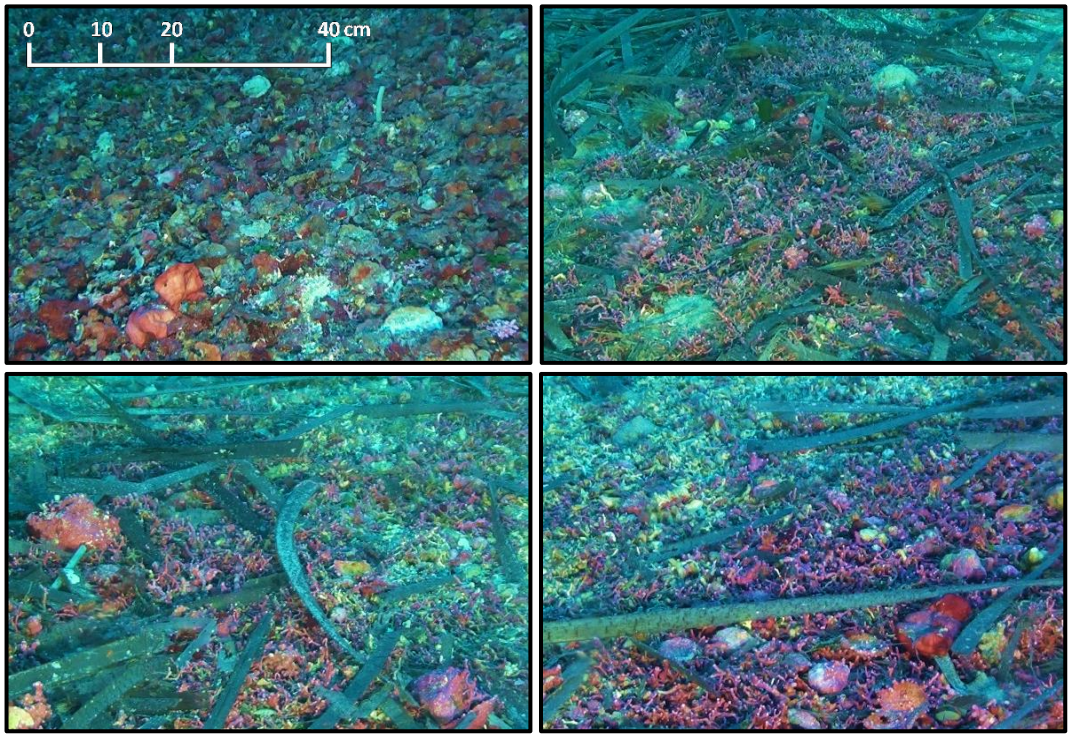

Figure 1. Example of rhodolith (maërl) beds, captured by ROV the from Pontine Islands study site. Extracted images from dives MS16_21 and MS16_128.

Their growth rate averages around 1 mm/year, but some species can reach 1.5 mm/year (Blake et al., 2003). With good environmental and nutritional conditions this continuously growing biogenic structure is capable of increasing the biological and functional diversity of coastal sediments. Their distribution depends on depth, hydrodynamic energy, substrate type, light and salinity concentration (Riosmena-Rodríguez, 2017).

Rhodolith beds provide essential habitat for a diverse range of marine species, including various invertebrates, fish, and algae. They offer refuge and nursery

grounds for juvenile organisms and support a complex web of ecological interactions (Foster et al., 2015). These species contribute to the production of carbonate in their tissues (in form of $CaCO_3$ and $MgCO_3$) which eventually becomes part of the seabed sediment (Johnson et al., 2013). This process can happen during their lifespan, when small pieces break down from the structure or when they die and decompose playing a role in the global carbon cycle.

The global carbon cycle is a dynamic system that regulates the flow of carbon between Earth's major reservoirs: the atmosphere, land, ocean, and biosphere. This cycle plays a critical role in regulating Earth's climate and maintaining the carbon balance essential for life. Marine environments, including the oceans and coastal ecosystems, are integral components of the carbon cycle (Henson et al., 2012), with a profound impact on carbon storage and the Earth's climate system (Falkowski et al., 2000) by regulation and storage. They act as a substantial carbon sink by exporting carbon from the surface ocean to the deep sea and dissolving atmospheric CO_2 at the ocean's surface. Coralline algae are sequestering and storing carbon, not just by photosynthesis, but also with calcification ($CaCO_3$ production) (Rendina et al., 2022). This process helps regulate atmospheric CO_2 concentrations, mitigating the effects of human-induced emissions (Lutz et al., 2007). Rhodolith beds can stabilize sediments, helping to prevent coastal erosion in some areas, by acting as natural breakwaters (Steller et al., 2016). They increase habitat complexity and benthic diversity (Amado-Filho et al., 2017), improving other, cultural ecosystem services, such as recreational fishing and diving (Niz et al., 2023). Understanding their role is crucial for addressing climate change and preserving marine ecosystems.

In Europe they occur throughout the Mediterranean, along most of the Atlantic coast from Portugal to Norway, and in the English Channel, Irish Sea and North Sea. The presence of rhodoliths and their role in the Mediterranean Sea has been documented by multiple scientific studies (Basso et al., 2017). In fact, the Mediterranean Sea is among the regions with the highest diversity of rhodolith forming-species (Rebelo et al., 2021).

Despite rhodolith beds in the Mediterranean Sea are as prominent as those in the Atlantic and Pacific region, and they build up an ecologically valuable, unique ecosystem in this semi-enclosed area, European rhodolith grounds suffer a variety of anthropogenic perturbations. Direct exploitation through extraction, fishing impacts and chemical pollution by organic matter and excess nutrients (Barberá et. al, 2003) being the most impactful ones. The size of rhodolith fundus area depends on the coverage of live algae, which can be decreased by muddying, epiphytism by soft algae and diffuse necrosis of structuring calcareous algae (Basso et al., 2015; Basso et al., 2018).

While identifying new rhodolith beds at unexplored locations, can be done using non-invasive methods, usually for the precise, taxonomical identification and characterization, direct collection of background samples is necessary (Rendina et al., 2020). After this this initial, destructive ground-truthing, long-term monitoring can be conducted with repeated ROV surveys or similar methods. These activities are ideally repeated on an annual basis, to show the state and possible changes of habitat conditions and distribution.

1.3. Acoustic survey techniques

Currently, there are two main types of equipment used in bathymetric studies, for the collection data about the seafloor morphology: single beam (SBES) and multi beam echosounder (MBES), the latter one gaining more popularity. While the single beam echosounders are widely used as practical surveying tools, their limited coverage (Schimel et al., 2010) and lower resolution (Wölfl et al., 2019) makes them less effective for detailed habitat mapping. Multibeam sonar systems consist of an array of transducers that emit multiple sonar beams simultaneously **(Fig. 2)**. These beams fan out from the transducer, covering a broad swath of the seafloor, instead of just a line, beneath the survey vessel. The system measures the time it takes for the sound waves to travel to the seafloor and return, allowing for precise depth calculations. By analyzing the return signals from multiple beams, researchers can create detailed bathymetric maps of the seafloor (Hughes, 2018). Multibeam sonar technology has evolved significantly over the years, with continuous improvements in both hardware and software. It offers several

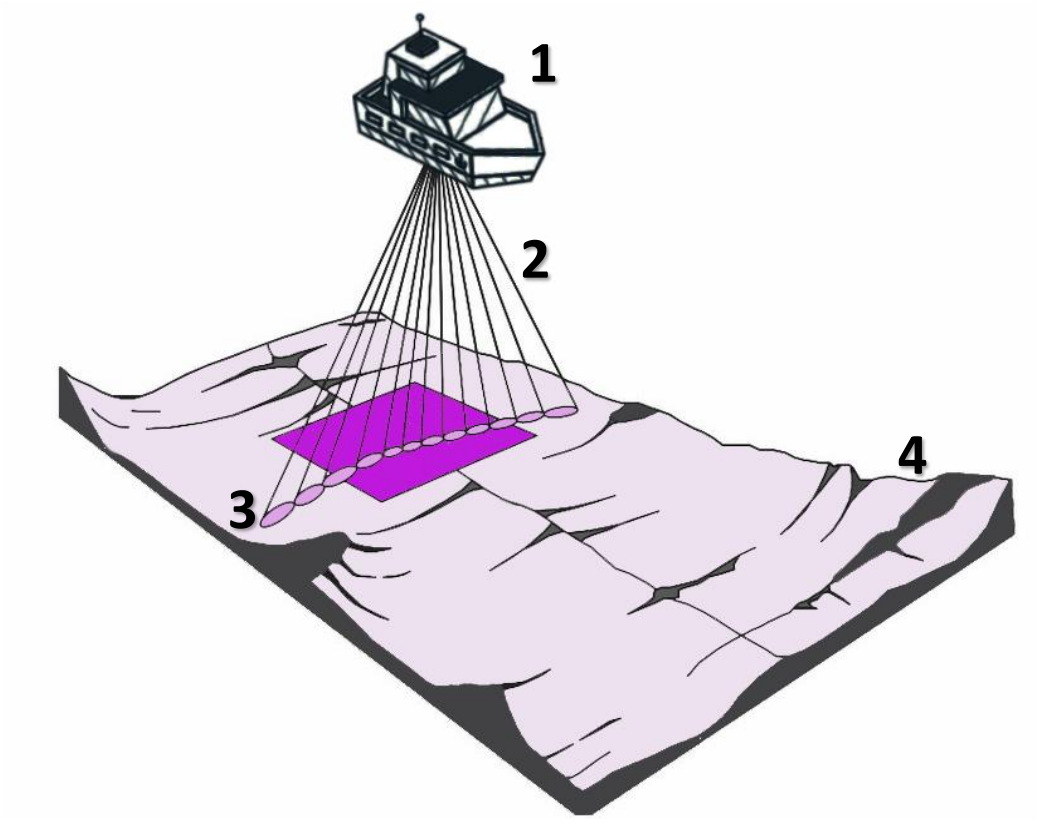

Figure 2. Minimalist diagram, showing the basic principles of surveying, with a multibeam echosounder. (1) platform to which the sonar is mounted, in this case a moving scientific vessel; (2) transducer emitted sonar beams, travelling towards the seafloor (before their reflecting back); (3) covered swath on the seafloor; (4) seafloor. Square shaped area in the middle (purple) representing a bathymetric tile, with a defined resolution.

advantages, including rapid data acquisition, wide coverage, and the ability to capture fine-scale seafloor features (Calder and Mayer, 2003). The size of the captured area depends on multiple factors, including beam widths, chosen opening angle and water depth. Using small angles in shallower water depths, generally results in higher resolution, while this decreases with increasing water depth (Lurton, 2002)

One advantage of multibeam echosounder is that it provides exceptionally high-resolution, fine-scale images of the seafloor, in a shorter time frame compared to SBESs (Wölfl et al., 2019). It is widely used in geological habitat mapping and environmental assessments. It enables scientists to locate and classify benthic habitats, which is essential for marine conservation and resource management (Lucieer et al., 2017). The technology also aids in the detection of changes in seafloor features over time, making it a valuable tool for monitoring environmental impacts.

Multibeam sonar plays a critical role, also in hydrographic surveys, ensuring safe navigation for ships and submarines by providing up-to-date depth information (Mayer et al., 2018). This technology is indispensable for maintaining navigational charts and ensures the safety of maritime transportation worldwide.

Ongoing advancement in multibeam sonar technology continues to expand its capabilities, including enhanced data processing algorithms, higher frequencies for improved resolution, and integration with other sensors and AUVs (Ånonsen and Hagen, 2010). These developments are expected to further enhance our ability to explore and understand the seafloor, benefiting both scientific research and practical maritime operations.

1.4. Using Remotely Operated Vehicles for data collection

Data collection in the marine environment presents unique challenges due to its depth, remoteness, and inaccessibility. Among the innovative tools available, Remotely Operated Vehicles (ROVs) have revolutionized many industries (McLean et al., 2020) and the field of marine biology, geology, archaeology, and environmental monitoring. They have been used for various scientific purposes, including benthic habitat research (Macreadie et al., 2018).

The concept of remotely operated vehicles for underwater exploration emerged in the mid-20th century. In 1953, a French engineer, Dimitri Rebikoff equipped a modified torpedo with adjustable cameras and operated it with cable connection for investigating shipwrecks (Yuh and West, 2001) thus creating the first ROV for sea exploration. In 1966, the US Navy developed the first Cable-controlled Undersea Recovery Vehicle (CURV), primarily designed for salvage operations (Talkington, 1983). These early versions were limited in their capabilities but laid the foundation for future generations. The 1980s and 1990s saw significant advancements in ROV technology. The introduction of compact and more powerful thrusters, better cameras, sensors and manipulator arms enhanced their capabilities. The 'Jason Jr.' ROV, developed in the mid-1980s by the Woods Hole Oceanographic Institution, played a central role in deep-sea exploration, including the discovery of the RMS Titanic wreckage (Ballard et al., 1995). Reaching the late 20th century, new innovations enhanced their utility for a wide range of marine science applications (McFarlane, 2001).

ROVs are capable of reaching extreme depths, enabling researchers to investigate the seafloor in remote locations that are otherwise challenging or impossible to access (Clark et al., 2010). ROVs are unmanned submersibles equipped with cameras, sensors, and manipulator arms. They can be programmed for certain tasks and operated remotely from the surface, offering researchers the ability to explore and collect data from the seafloor in real-time. ROVs can operate continuously for extended periods, facilitating comprehensive and systematic surveys of benthic habitats. With the help of cameras, they provide detailed images and high-resolution videos of the seafloor, suitable for the identification of benthic species and substrate types (Watling et al., 2013), as well as oceanographic parameters (temperature, salinity, acidity, etc.) according to the sensors installed on them. ROVs have also been employed to acquire multi beam data, orthophoto mosaic and hyperspectral data, by installing MBES, camera or hyperspectral camera underneath them, respectively (Lim et al.,2018; Foglini et al., 2019). Involved in various monitoring activities, ROVs with their capabilities, can help to evaluate the impact of human activities on benthic ecosystems, particularly in regions subject to higher anthropogenic disturbances (Levin et al., 2019). Their non-invasive approach allows critical research conducted on sensitive species while minimizing environmental impact (Chimienti et al., 2018).

Moreover, ROVs equipped with specific sensors, robotic arms or special containers can collect samples of sediments, fauna, and flora, enabling detailed biological and chemical analyses (Lindner et al., 2008). These methods, although considered invasive, significantly contributed to the discovery of new species and the documentation of biodiversity in previously unexplored deep-sea habitats.

The ongoing development of ROV technology, including advanced imaging systems and autonomous capabilities, promises even greater contributions to benthic habitat studies. More recent developments include the use of autonomous ROVs (AUVs), which can operate independently covering large areas, without real-time human control. They are usually pre-programmed for completing certain tasks, following a defined route, closer to the seafloor. These AUVs are valuable for collecting data in large, challenging or extreme deep-sea environments (Wynn et al., 2014).

1.5 Aim of the study

By utilizing the capabilities of both acoustic technology and ROV imagery, this thesis contributes to map the distribution of substrate and rhodolith beds of the Pontine Islands (Northern Tyrrhenian Sea, Italy), constituting the base for future monitoring activities of the GES of this critical marine ecosystem.

In the following sections, the methodology **(Fig.6)** employed for creating a benthic habitat map **(Fig.7)** is described, showing the results of data acquisition **(3.2)**, processing **(3.2)** and classification **(3.4)** efforts. Highlighting also the practical implications **(5)** of new findings for marine conservation and resource management.

2. Study area

The study focuses on a distinct area, located in the Northern part of the Tyrrhenian Sea, Italy **(Fig.3)** The Tyrrhenian Sea is a part of the Mediterranean Sea and is situated in the Western Mediterranean Basin. It is surrounded by the Italian Peninsula to the east, the islands of Corsica and Elba to the north, the island of Sardinia to the west, and the islands of Sicily to the south. With a surface area of roughly 275.000 km², it represents the largest sea in Italy as well as the third-largest marginal sea as part of the Mediterranean Sea. It exhibits a diverse bathymetric profile, with depths ranging from shallow coastal areas to deeper basins. The northern Tyrrhenian Sea tends to be shallower, with depths averaging around 200 to 800 meters. In contrast, the central and Southern parts feature deeper basins, with some areas exceeding 3,500 meters in depth (Palmiotto and Loreto, 2019). It is divided into two basins (or plains), the Vavilov plain and the Marsili plain, where the large undersea volcano, the Marsili seamout can be found (Ventura et al., 2013). They are separated by the undersea ridge, known as the Issel Bridge.

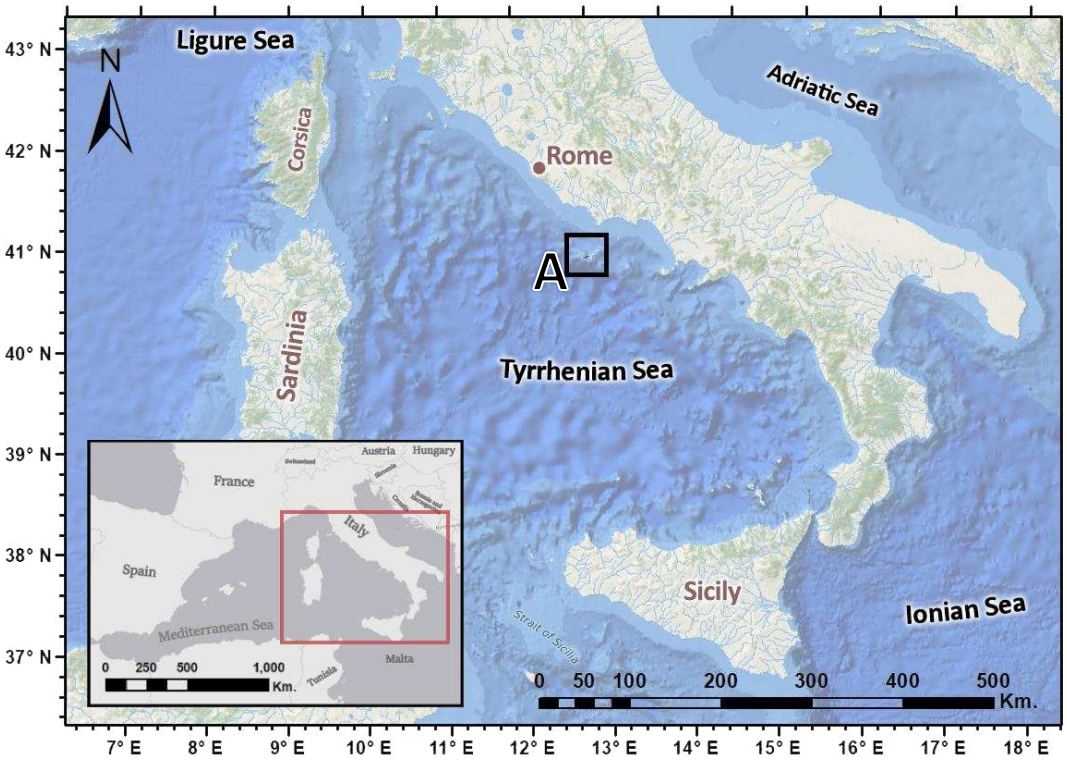

Figure 3. Map of the Tyrrhenian Sea, with a general EMODnet Bathymetry Digital Terrain Model layer, highlighting the location of the study area (A) Pontine Islands.

The Tyrrhenian Sea experiences a complex system of ocean currents influenced by both local and regional factors (Iacono et al., 2021). The Corsica Channel, located between Corsica and the Italian mainland, is a significant passage for water exchange between the Ligurian Sea and the Tyrrhenian Sea. The Tyrrhenian

Current flows along the Western coast of Italy, entering from the Ligurian Sea to the north. It then circulates southward along the Western coast, bringing relatively cooler, nutrient-rich water. In the Southern Tyrrhenian Sea, the Atlantic Ionian Stream (AIS) merges with the Tyrrhenian Current. This combined current (also called Tyrrhenian Cyclonic Circulation) flows eastward, impacting the Eastern coast of Sicily and contributing to its unique hydrodynamic conditions (Millot, 1999). Seasonal variations in currents, influenced by atmospheric conditions, play a crucial role in this localized circulation pattern, while contributing also to the Mediterranean Sea's (Artale et al., 1994).

The Tyrrhenian Sea holds great ecological and economic importance. It is a critical habitat for a variety of marine species, including commercially valuable fish and molluscs. The seafloor's diverse topography and habitats, ranging from sandy plains to rocky reefs, support rich biodiversity (Bianchi et al., 2017). The region is also a popular destination for tourism and recreational activities due to its stunning coastline, historical sites, and mild climate. Many coastal communities depend on fishing and tourism, making sustainable management of the Tyrrhenian Sea's resources essential for their livelihoods (Danovaro and Boero, 2019).

The study area is located at the Northern sides of the Tyrrhenian Sea, between Palmarola and Ponza Islands, offshore central Italian coast. Hereby referred to it collectively as the Pontine Islands.

2.1. Pontine Islands

The Pontine Islands (or *Isole Ponziane*) are a group of Islands in the Tyrrhenian Sea, as part of the Lazio region. The archipelago includes six islands with various sizes, the three largest being Ponza, Palmarola and Ventotene.

The Pontine Islands and the surrounding seafloor are under different levels of protection **(Fig.4)**, following the requirements of the Habitat Directive 92/43/CEE. Palmarola, Ponza and Zannone islands and their sorroundings, are considered a Special Protection Zone (SPZ), and are listed among the Natura2000 sites (IT6040019), with the names: "Fondali circostanti l'Isola di Palmarola - IT6000015", "Fondali circostanti l'Isola di Ponza - IT6000016", "Fondali circostanti l'Isola di Zannone - IT6000017".

Ventotene and Santo Stefano are protected by the 'Ventotene and Santo Stefano Islands Marine Protected Area (MPA)' where fishing and catching of any living species are forbidden (Italian Ministry of Environment, https://www.mase.gov.it/)

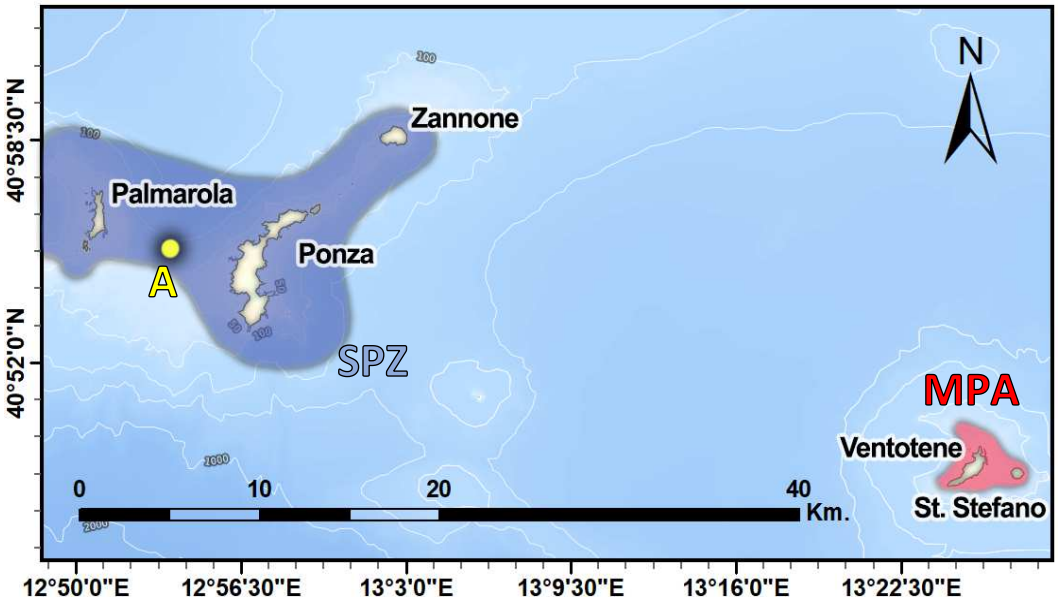

Figure 4. Map of Pontine Islands, showing the location of the study area (A - yellow dot), the Special Protection Zone (SPZ-dark blue area) and the Ventotene and Santo Stefano Islands Marine Protected Area (MPA - red area).

Several marine communities were discovered in recent years, in the area. As an example, black coral forests near the Western islands (Ingrassia et al., 2016) or *Isidella elongata* (Esper, 1788) bamboo coral colonies (Ingrassia et al., 2019) at the north-western parts. The presence of *Posidonia oceanica* (Delile, 1813) meadows, at multiple locations are also reported and adds to the natural values of the coastal and marine ecosystems (Raimondi, 2014). The mainly volcanic islands (Chiocci and Orlando, 2004) are surrounded with small rock formations (Italian: *formiche*) which can also enhance biodiversity, providing hard substrate for sessile and shelter for mobile organisms.

Acoustic and archaelogical surveys, in small areas and with and various bin sizes (2-10 m) were conducted in the area (Ingrassia et al., 2019; Ritondale, 2014) but many of them were focused more on peculiar species or on smaller areas, with already documented interests, as opposed to large-scale substrate and habitat mapping.

3. Materials and Methods

3.1. Data Collection

The seabed located between Palmarola and Ponza Islands was investigated in 2016 by the National Research Council (Italian: Consiglio Nazionale delle Ricerche, CNR), within the framework of the MSFD. Geophysical (multi beam) data and seabed samples (ROV images and grab samples) were collected **(Fig. 5)**.

High-resolution multibeam data were collected between the 15th of July and 5th of August 2016, with a Teledyne Reson Seabat 7160 multibeam echosounder, mounted on the R/V 'MINERVA UNO', and covered an area of 15.4 km^{2}, using 5x5 m pixel size A predetermined, optimal route was followed, covering 100% of the area, with overlapping transects for multi beam soundings. Accurate positioning was obtained by means a GPS system, vessel motion was corrected through a motion sensor unit installed within the MBES and sound velocity into the water was periodically acquired to correct acoustic data.

The ROV (Remotely Operated Vehicle) images were collected using a Pollux III, which has a maximum operating depth of 600 m. The ROV was equipped with a CCD (low definition) camera used for navigation and transect analysis and with a SonyHDR-HC7 high-definition camera, used for species' identification and further studies. Both cameras were associated with LED lamps as light sources, ensuring better visibility. Three ROV dives were conducted, investigating a seabed area of 9,5551,19 m^{2} (9.5 x 10^{-3} km^{2}) in total, corresponding to 0.062% of the acoustic survey area **(Tab.1)**.

Dive ID	Starting location Lat N – Long E	Ending location Lat N –Long E	Min. depth (m) – Max. depth (m)	Length (m)	Covered area (m^{2})	Date	Hour (UTC)
MS16_21	40.91 N – 12.88 E	40.92 N – 12.89 E	60.06 – 62.93	1203.35	3610.05	18/07/2016	07:35 09:27
MS16_128	40.91 N – 12.87 E	40.91 N - 12,87 E	44.21 – 58.02	793.26	2379.78	27/07/2016	08:19 09:55
MS16_142	40.91N – 12.91 E	40.91 N – 12.90 E	51.38 – 69.77	1187.12	3561.36	27/07/2016	16:01 17:46

Table 1. Table summarizing the detailed information about the dives MS16_21, MS16_128 and MS16_142, mostly focusing on their locations and travelled distances.

Finally, a total of 15 grab samples were collected using a Van Veen bucket from 5 different locations, along the track-lines of the ROV dives, with 3 replications at each site (according to the MSFD sampling protocols). They allowed a precise characterization of sediment types and rhodolith bottom **(Tab.2)**.

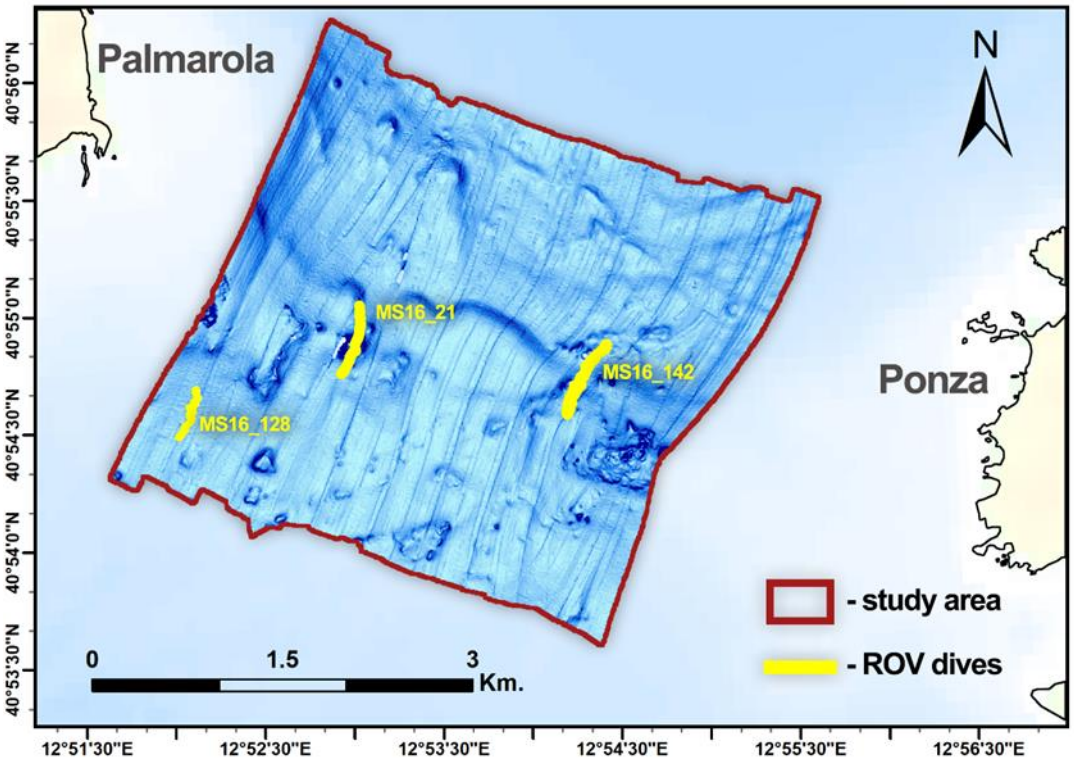

Figure 5. Map highlighting the study area (blue rectangle with red border), including the three ROV dives (yellow track lines).

Sample ID	Sampling point location	Depth (m)	Bucket fullness (%)	Substrate	Biology
MS16_132	40.91 N - 12.87 E	66.6	50	bioclastic sand	*Posidonia* leaves
MS16_133	40.91 N – 12.87 E	66.9	33	sand with rhodolith	rhodolith
MS16_134	40.91 N – 12.87 E	66.9	50	sand with rhodolith	rhodolith
MS16_135	40.92 N – 12.89 E	65.9	50	-	rhodolith branches
MS16_136	40.92 N – 12.89 E	66.4	50	-	rhodolith branches
MS16_137	40.92 N – 12.89 E	66.1	33	-	rhodolith branches
MS16_138	40.91 N – 12.89 E	37.2	33	-	bioconstruction pieces green algae (cf. *Caulerpa*)
MS16_139	40.91 N – 12.89 E	65	33	-	rhodolith branches
MS16_140	40.91 N – 12.89 E	64.9	25	-	-
MS16_143	40.91 N – 12.91 E	76.1	25	-	-
MS16_144	40.91 N – 12.91 E	76.1	33	-	rhodolith branches
MS16_145	40.91 N- 12.91 E	76.1	33	-	rhodolith branches
MS16_19	40.91 N – 12.89 E	65	25	-	-
MS16_20	40.91N – 12.89 E	65	-	coarse sand	rhodolith branches

Table 2. Table summarizing the detailed information about the grab samples collected at the Pontine Island study site with two (substrate and biology) levels.

3.2. Data Processing

In the following sections, the detailed methodology is described, on how the data was refined for a ready to use format for benthic habitat mapping purposes, including also the software and tools utilized in the procedure **(Fig. 6, Fig.7)**.

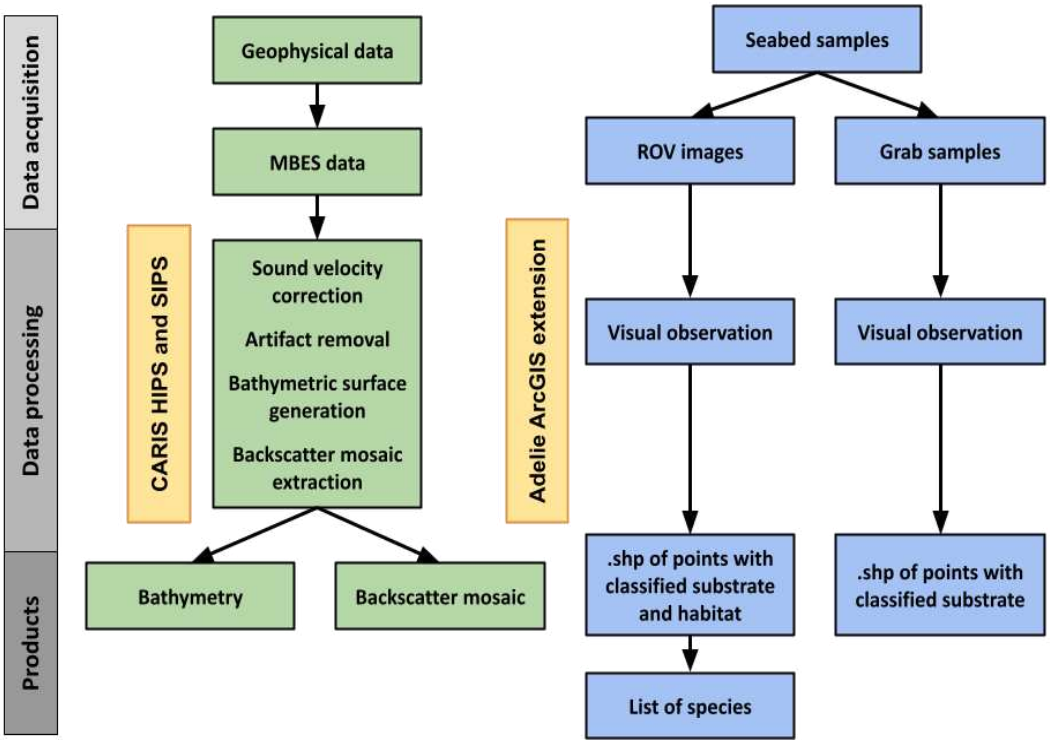

Figure 6. Schematic diagram, visualizing the workflow followed by the study (direction of arrows) to derive products from data acquisition. Green (geophysical data processing) and blue (seabed sample processing) rectangles represent specific steps and products, while yellow rectangles highlight software and tools used for those processes. Grey rectangles show the stages of processing.

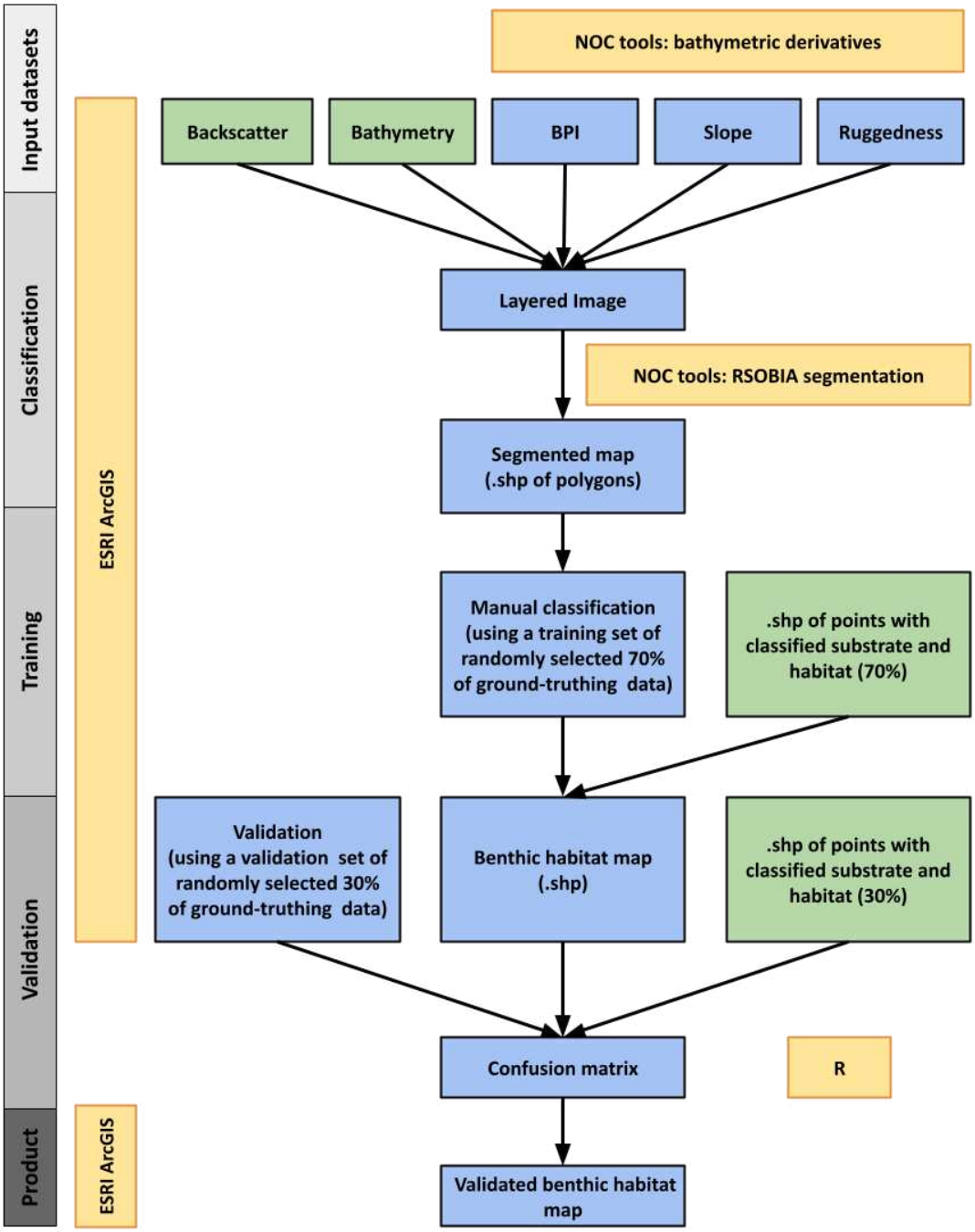

Figure 7. Schematic diagram, visualizing the workflow followed by the study (direction of arrows) on using the obtained data for the creation of a validated benthic habitat map. Blue rectangles represent specific steps and products, green rectangles present data already obtained from previous stages, while yellow rectangles highlight software and tools used for those processes. Grey rectangles show the stages of processing.

3.2.1 Acoustic data processing: bathymetry and backscatter

The multi beam data acquired are in *.s7k* format and were processed using CARIS HIPS and SIPS 11.0 software, with the aim of correcting positioning and sound velocity errors and removing artifacts to produce a bathymetric surface and an acoustic backscatter mosaic.

The raw multibeam lines were imported into CARIS HIPS and SIPS through the appropriate wizard, that converted the lines into a format readable from the software. The sensor data import automatically corrected the data for the sound velocity, by reading the sound velocity profile acquired during the survey and applied during the acquisition. Afterwards, they were "georeferenced" correcting them also for the tide: a 'zero tide' file was used, since at the location the tide was so low, that did not affect bathymetric acquisition.

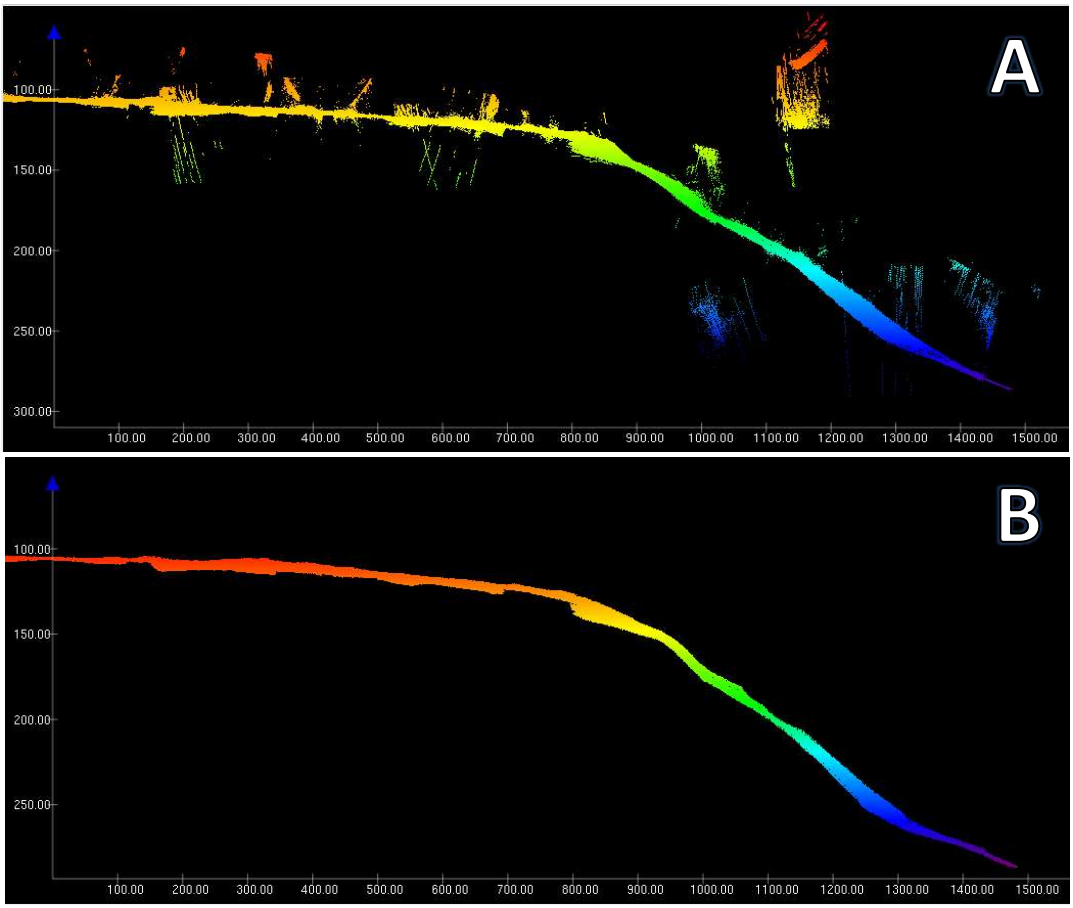

Figure 8. Subset of the seafloor, shown from a horizontal view. Before cleaning (A) and after cleaning (B). Vertical scale (in meters) shows depth, horizontal scale (in meters) shows length of the segment.

Subsequently a bathymetric surface, with a horizontal spatial resolution of 5 m was created and manually analyzed for artifacts and spikes using the 'Subset editor' tool that allows the user to analyze the data slice-by-slice **(Fig. 8)** Cleaning soundings

from artifacts manually has both disadvantages and advantages. It is time consuming and introduces subjectivity to the process, but it is affordable for small dataset and relies on scientific expertise in discriminating among errors and real features, contrary to automatic algorithms. The result of this phase is a 5 m-resolution surface bathymetry that can be used for further analyses.

Afterwards, the acoustic backscatter mosaic was extracted from raw data by means of the SIPS backscatter algorithm, available in 'New SIPS Mosaic' tool of CARIS HIPS and SIPS. The mosaic was corrected for the depth and the morphology using the processed bathymetry **(Fig.9)**.

The results are two ASCII files, one for bathymetry (and one for acoustic backscatter, then converted into ESRI grid using ESRI ArcGIS 10.7.

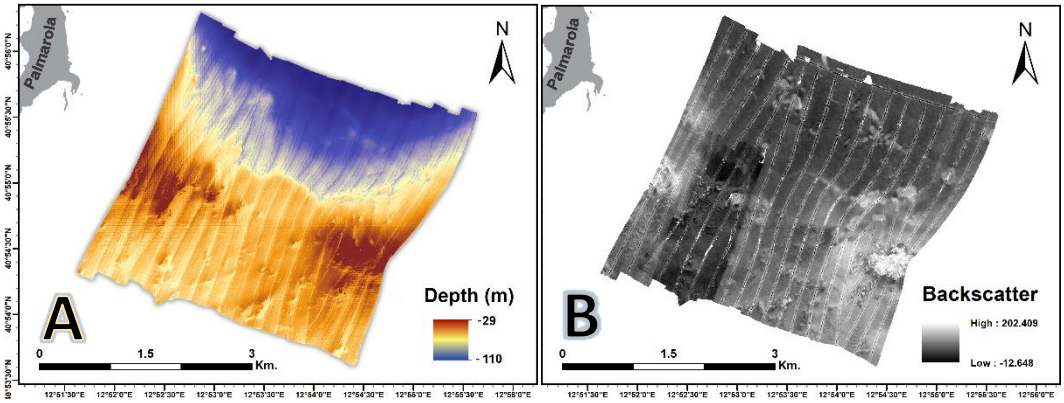

Figure 9. Results of the acoustic data processing. Maps showing the bathymetry (A) and the acoustic backscatter (B).

3.2.2 Processing ROV videos

A total of 3 dives, conducted at the Pontine Islands were analyzed: MS16_21, MS16_128 and MS16_142 **(Tab. 1)**. During each dive the ROVs precise GPS location (coordinate reference system: WGS84) was recorded, continuously in every 2s. The navigation tracks were smoothed using Adelie GIS, a tool of *Adelie* software (©IFREMER) for *ArcMap*.

The first dive, MS16_21, with a length of roughly 1200 meters, had a duration of 102 minutes (from 07:35 UTC to 09:17 UTC) from which 676 picture was obtained and analyzed.

The second dive, MS16_128, with a length of roughly 790 meters, had a duration of 96 minutes (from 08:19 UTC to 09:55 UTC) from which 580 picture was obtained and analyzed

The third dive, MS16_142, with a length of 1187 meters, had a duration of 105 minutes (from 16:01 UTC to 17:46 UTC) from which 638 picture was obtained and analyzed.

The videos were georeferenced using *Adelie Video* (©IFREMER) and a frame from every 10 seconds was extracted from each video. The following attributes were obtained by analyzing frames:

The video material was analyzed by selecting a still image from every 10 seconds of each video, using *Adelie Video* software made by *Ifremer*, which automatically linked the images to their geographical coordinates, from the navigational file. For each examined frame (1894 in total) the following attributes were obtained, describing the seafloor and benthic habitat:
-substrate type and its coverage in percentage
-macroscopic sedimentary structures present on the substrate
-benthic species, classified to the lowest taxonomical rank possible
-number of individuals
-presence of human impact

The specific substrate types were visually identified, if the visibility was adequate enough. In cases where the substrate was not identifiable, the last good quality image was taken into consideration.

The coverage of the different substrates and habitats at a given image were also visually determined, using a virtual grid, which split up the images into equal parts, thus helping to determine the closest possible percentage value. Despite the fact, that statistical calculation wasn't conducted on the precision of this approach, it was suitable for the aim of finding the dominant substrate and habitat type at each image **(Fig. 10)**.

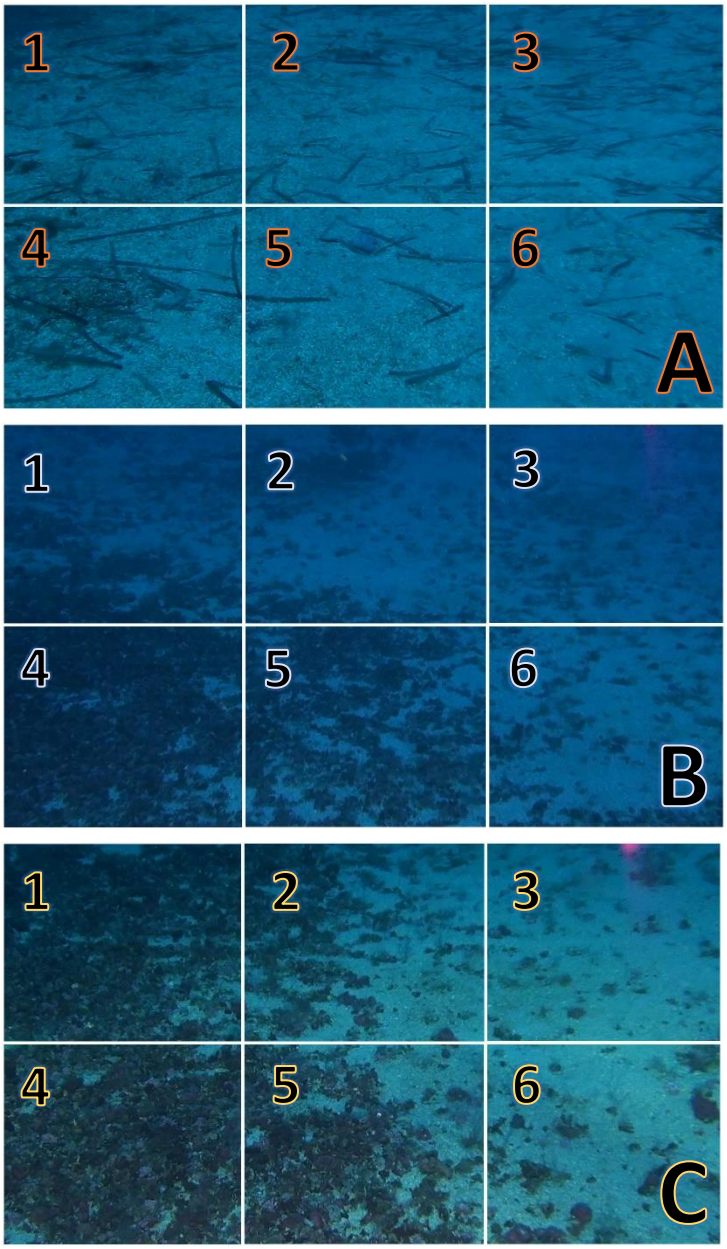

Figure 10. Visual representation of the grid system method, used for the ROV images' coverage calculation. By adding together, the separated parts own coverages, the entire coverage on the frame can be calculated more precisely. The segment A/6 contains 100% bioclastic sand, on the segment B/4 rhodolith is covering 90% of the substrate, while on the segment C/5 this number is around 60%, etc. The final coverages on the images became: (A) 90% bioclastic sand - 10% rhodolith; (B) 65% fine unconsolidated substrate - 35% rhodolith; (C) 55% bioclastic sand - 45% rhodolith. While these numbers can be estimated only approximately, this method is adequate enough to decide which is the dominating substrate and habitat on the given image.

3.3. Remote Sensing Object-Based Image Analysis (RSOBIA)

Using RSOBIA segmentation, a thematic map can be created, by aggregating pixels together. The tool is taking multi-layered images as input and considering the statistic associated with the layers, creates a set of polygons as output. These clusters are further combined to create classes. This clustering process works according to the minimum polygon size rule and other clustering rules (Le Bas, 2016). To a successful segmentation, the user needs to define three parameters. The (1) number of clusters, depending on the complexity of the data and general purpose; (2) minimum object size, which defines the minimum output polygon size; if the user decides that one layer is more important or has better quality then the other(s), specific (3) layer weights can be used (Le Bas, 2016). This semi-automated, object based, image analysis (OBIA) is among the most widespread methods used to produce reliable habitat maps for various purposes (Prampolini et al., 2021). In many surveys, multiple echosounder systems are used, resulting in different acoustic reflectivity datasets, which are often not calibrated. In these cases, RSOBIA can be a good option, because it's based on objects, rather than on pixels (Prampolini et al., 2021). Moreover, it is a user-friendly, freely available, open ArcGIS extension.

From the many obtainable terrain attributes, slope, aspect, curvatures and other measures of seabed roughness have all been used in habitat mapping studies, but making a subjective choice of variables may reduce map accuracy and produce maps that do not adequately represent habitats and species distributions (Lecours et al., 2016). In this study the bathymetry, backscatter, BPI, slope and ruggedness variables were found to be the most efficient, in combination for RSOBIA segmentation. They're the best at describing the seabed morphology in this area, with its spatial resolution. The terrain attribute layers were converted into layered images (.img) as data IMPUT layers for segmentation. After trials, testing the most optimal cluster number, 15 clusters were chosen **(Fig.22)**, with a minimum object size of 50. With this pixel size (5 x 5 m) it is best in considering more local features on the seafloor, therefore it was suitable for the scale at which the benthic habitat maps were planned to be created **(Tab.4)**. By visual interpretation of test segmentations, trying the different attributes' relative weight combinations and considering that backscatter data is powerful in sediment differentiation, this attribute was given three times more weight, compared to the others. Consequently, the final coded layer weight parameters were set to: 3,1,1,1,1 (Backscatter, BPI, Bathymetry, Slope, Ruggedness).

3.3.1. Terrain attributes used for segmentation

Slope

Slope **(Fig.11)** is a first order derivative of the bathymetric surface. It shows the maximum slope of every surface in degrees, ranging from 0 (completely horizontal) to 90 (completely vertical). A study from 2007, reviewing research papers on habitat mapping, showed that more than half of them used slope as one of their predictors for classification (Wilson et al., 2007). It can be applied on wide range of terrain complexity, and can be computed easily on many widely available GIS software. In comparative studies on optimal terrain attribute selections, slope was among the most recommended ones, performing well across environmental studies (Lecours et al., 2017). While slope computations are popular and widely available there is a great variation in the obtained values due to differences between the applied algorithms and resolution or analysis scale (Dolan & Lucieer, 2014). Moreover, performance and accuracy of the estimation methods may vary under different terrain conditions, landscapes and other parameters (Warren et al., 2004). The Benthic Terrain Modeler tool, installed on ArcMap 10.7 was used to calculate slope. This algorithm uses the method of Horn, with 3x3 neighborhood cell range (also known as Moore neighborhood) on a planar surface (Walbridge et al., 2018).

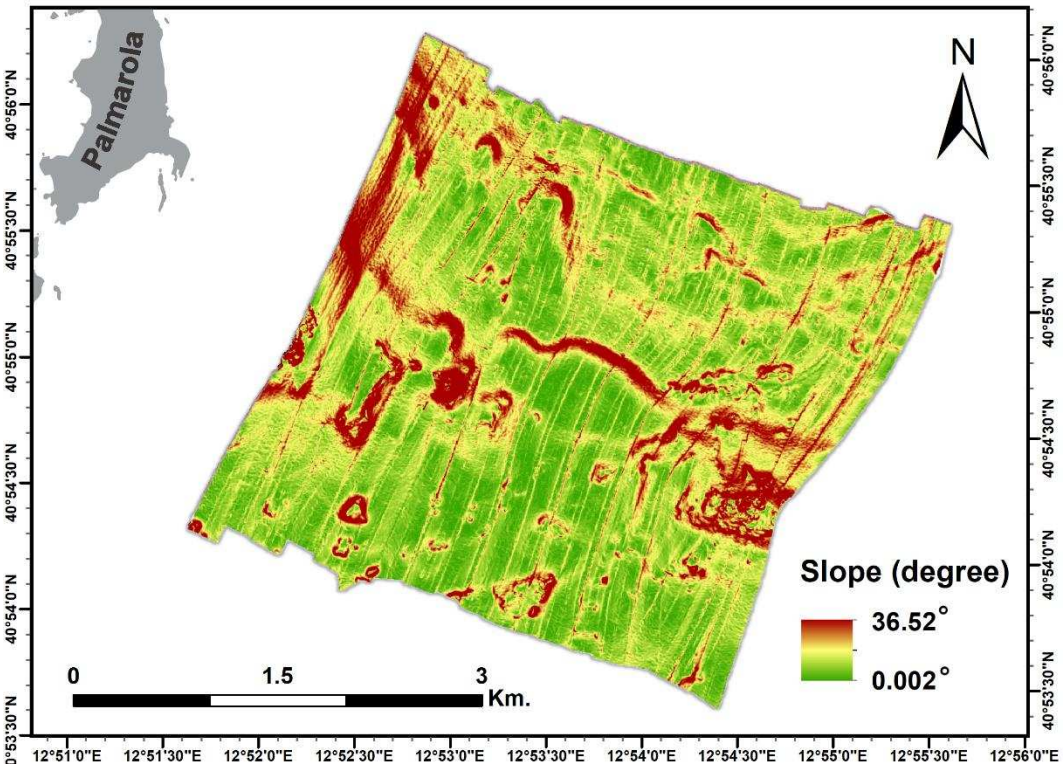

Figure 11. Map showing the slope, derived from multibeam bathymetry, with a resolution of 5x5 m. Colours indicate the steepness of the seafloor: darker colours indicate higher degrees of inclination (the highest being 36°) at certain locations, while brighter colours highlight the mostly flat areas.

BPI

To further identify different, small-scale crests and depressions present on the seafloor, a secondary derivative need to be used. The Bathymetric Position Index (BPI) **(Fig.12)** is based on the Topographic Position Index (TPI) originally proposed by Weiss (2001). The BPI calculating algorithm utilizes a neighbourhood analysis function to measure elevation variations between a focal point and the mean elevation of surrounding cells, within a user-defined area. Usually a negative BPI value indicates a cell lower than its neighbours (i.e., a depression), while a positive value signifies a cell found higher than its surroundings (i.e., a crest). Flat or consistently sloping areas receive near-zero values (Micallef et al., 2012). Knowing that the precise settings of a BPI calculation can be modified by an expert, for specific case uses, the achieved final BPI map, can represent the seafloor alterations in a very high-resolution format. Sometimes they can include features that are otherwise difficult to discern by eye or from bathymetric data. The classified habitat maps, using BPI as one of their main predictors, can be more consistent and provide an objective approach to unsupervised classification (Verfaillie et al., 2007).

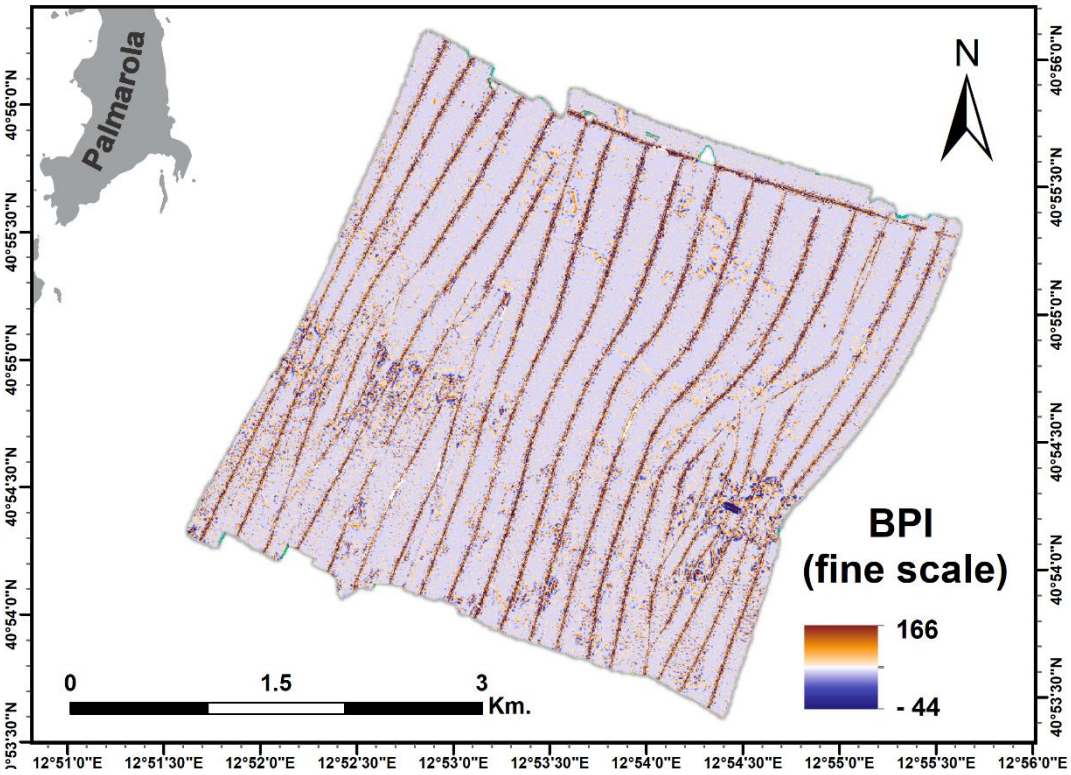

Figure 12. Map showing the Bathymetric Position Index calculated on the study area. The fine scale BPI map indicate zones with higher variations among the position of neighbouring pixels. Locations with varying colours indicate more depressions and elevations in small ranges, while unicoloured regions are considered mostly flat.

Ruggedness

The ruggedness **(Fig.13)**, a widely used terrain attribute (Calvert et al., 2015), measures of seabed complexity, by quantifying the topographic heterogeneity (Riley et al., 1999). It is also called rugosity, and it calculates the variability among neighboring cells. It considers the slope and aspect, as important factors as well (Le Bas, 2016) further enhancing its precision and usefulness.

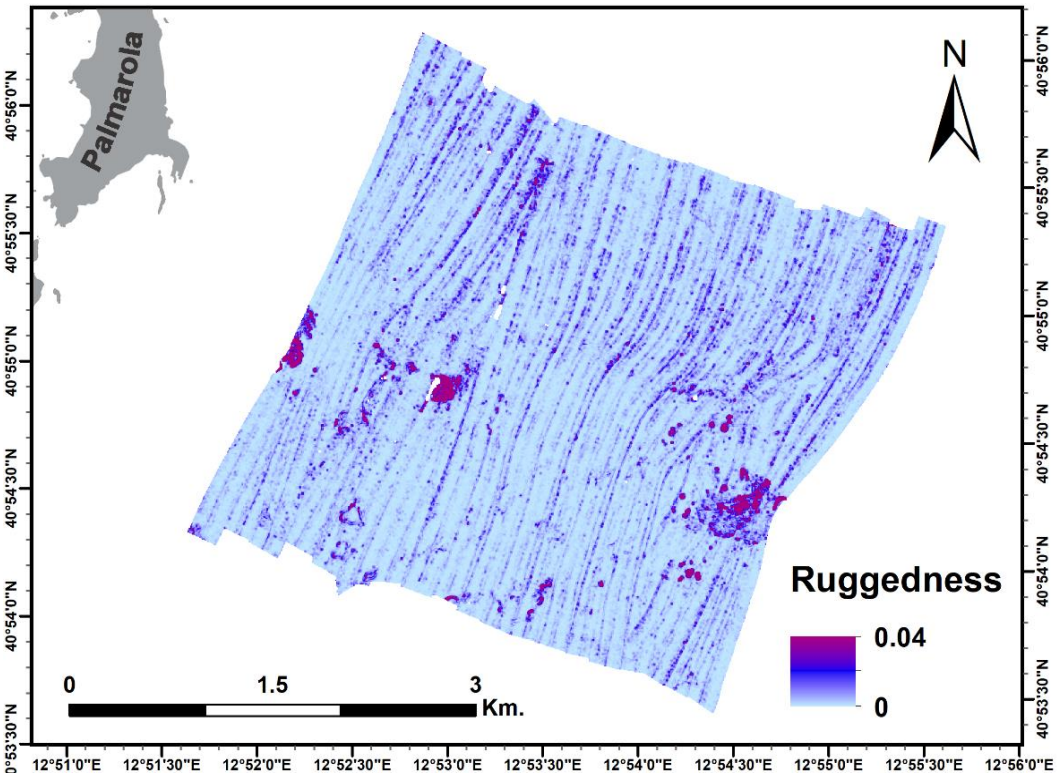

Figure 13. Map showing the ruggedness, derived from multibeam bathymetry, with a resolution of 5x5 m. Colours indicate the complexity of the seafloor: darker colours indicate areas with more heterogenous terrain, while brighter colours show homogenous locations.

Backcatter

Acoustic backscatter **(Fig.14)** is the acoustic signal retro-diffused by the seafloor towards the multi beam receivers and is widely used in marine geology and habitat mapping studies. The strengths of this signal are strictly related to the nature and texture of seafloor sediments and habitats. For example, fine sediments exhibit distinct backscatter patterns compared to coarse sediments (Alevizos et al., 2018). This information assists in identification of different sediment types, composition and structure, as well as benthic habitats (e.g. *Posidonia oceanica* meadows, coralligenous and bioconstruction organisms, rhodolith beds), based on their acoustic response. The backscatter data, ideally combined with other attributes can be used for habitat mapping, to predict the distribution of benthic organisms and understanding their relationship with the seafloor (Brown et al., 2011).

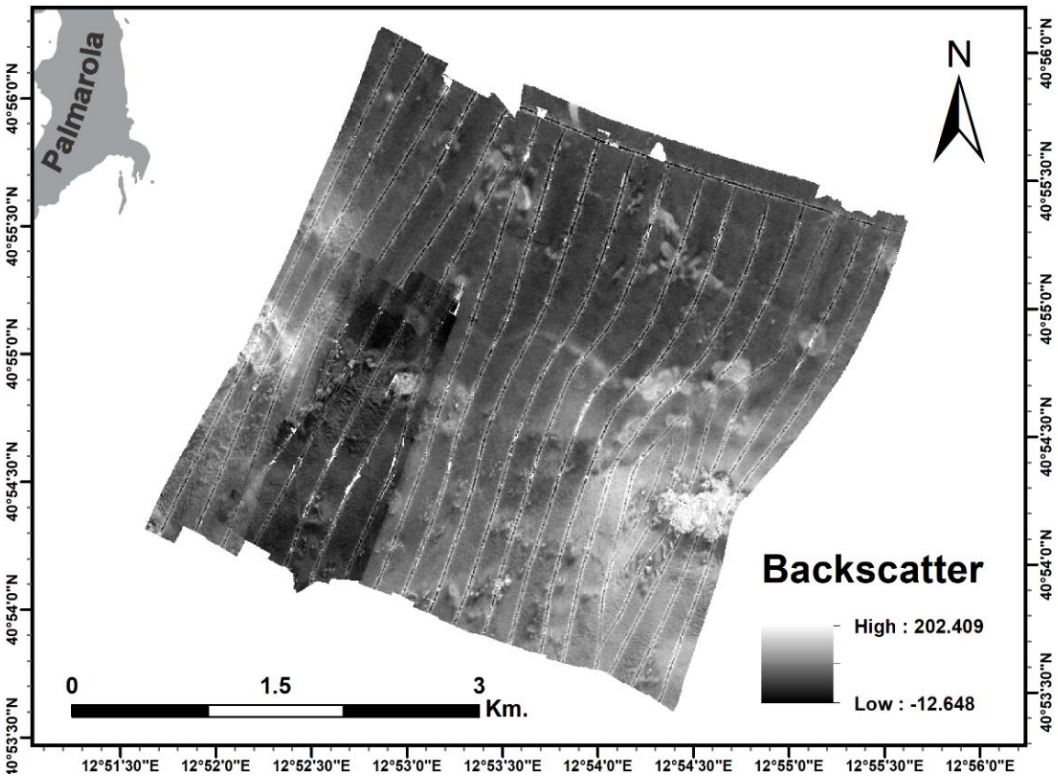

Figure 14. Backscatter data obtained on the study site, with a 5x5 m resolution. Dark colours indicate lower reflectivity, suggesting the presence of soft or muddy bottoms, while bright colours indicate high reflectivity, suggesting the presence of hard bottoms, rock formations and possibly rhodolith beds.

3.4. Classification

To ensure the most precise habitat classification possible, a consistent approach should be used.

For this study the CoDeMap Habitat Classification Scheme (HCS) was used. It was developed specifically for the Mediterranean and Black Seas within the framework of the European Project CoCoNet (Boero et al., 2016) and still under review, but already successfully applied in benthic habitat mapping (Angeletti et al., 2019; 2020; Prampolini et al., 2020) It categorizes benthic habitats, by capturing their three main components: morphology, substrate and biology (Kostylev et al., 2001; Diaz et al., 2004; Romsos et al., 2007). In the hierarchical structure each component has three levels, starting from a general one, which identifies coarser features, a fine-scale level can be reached, which captures even the finest details. Each item at each level has a univocal code and they can be combined for precise identification and, if the features are completely distinct, multiple codes can be used at the same time (in these cases they're separated with a '+' sign). Some examples from a not yet published article include: P02G0902BF05 indicating a sediment wave (BF05) on a canyon flank (G0902) on a continental slope (P02), or B090737, which stands for a coralligenous (B0907) bioconstruction (B09) with massive sponges (B090737).

This flexible scheme allows to map each habitat component separately, producing morphological, substrate and species distribution maps, or together constructing abiotic surrogates (morphology + substrate components), or a full benthic habitat map (showing all the components). In this work, the attention was focussed on the substrate and biology components. A proper name of substrate and biology was given to each sample.

From the RSOBIA segmentation **(3.3)** a map was derived, separating 15 classes of possibly different substrate and biological components. To name the classes **(Fig.19)**, and later use them to construct substrate and habitat maps **(Fig.20)** ground-truthing data needed to be used. To predict the substrate and habitat types present in the classes a random selection of 70% of points with ground-truthing data (ROV images) were used during the training procedure. With the proper codes, describing each sampling point, it is possible to count, how many of a specific type falls inside one or another class. As an example, if a Majority class, contains 20 ground-truthing points, from which 5 shows rock substrate, 5 shows sand substrate and 10 shows bioclastic sand substrate, the latter will be used for naming that class, because it is present in larger quantities compared to any other type, in that area. If multiple substrate and habitat types are present in the same number, following, the same 20 points example: 10 contains sand, while the other half contains rhodolith bed as biological component, mixed classes can be created,

with the name: sand with rhodolith bed. Another example is shown on the **Figure 15** where two substrate types were classified, following the same methodology.

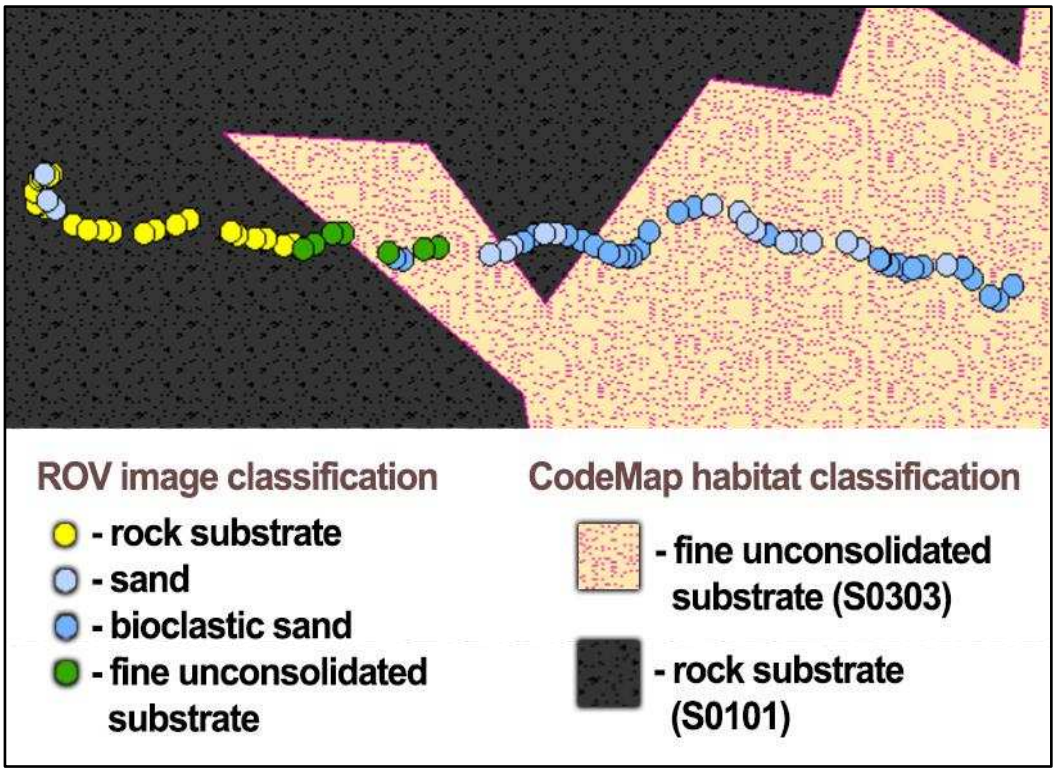

Figure 15. Example of substrate classification, highlighting a short section from the dive MS16_21. Coloured circles, representing image ground-truthing points from ROV video footage, indicating the dominant substrate type present at their position. In the background two major substrate types (classes) are defined by the number of matching sampling points inside their boundaries. In this case the sand (light blue) and bioclastic sand (pacific blue) substrate types were present in the area, but in smaller numbers than the fine unconsolidated substrate (green) and rock (yellow) substrates, so they're not showing up on the final classification of this specific area.

3.5. Validation

The accuracy assessment of the benthic habitat map in **Figure 20** was conducted by producing a confusion matrix, that compared the remaining 30% of ground-truthing, seabed samples with the predicted class in which they fall (both classified with the CoDeMap habitat classification scheme). Where the predicted class did not have a sample of the validation set falling in that area (e.g. the classes S030301 Sand and S030313 Gravelly sand), the classes were not included in the validation procedure, instead they were verified through comparison with other maps produced by public institutions, such as the CARG Sheet 413 'Borgo Grappa e Isole Ponziane'. Afterwards, the accuracy assessment procedure here presented was run for the classes S0101 Rock substrate, S0303 Fine unconsolidated substrate, and S030302 Bioclastic sand **(Tab.3)**.

4. Results

4.1. Morphological and acoustic backscatter characteristics

The seafloor **(Fig.16)** of the study area is relatively flat, with depths ranging between -29 and -110 m. The southern part of the surveyed area is shallower than the northern and characterized by bedrock outcrops with an irregular shape, highlighted also by the slope **(Fig.11)**, BPI **(Fig.12)** and the ruggedness **(Fig.13)**.

The acoustic backscatter **(Fig.14)** shows a southern part characterized by middle-high values of acoustic reflectivity of the seabed with patches, irregular in shape, of very high values. The northern part of the dataset is characterized by middle-low values of acoustic reflectivity with irregular patches of high reflectivity values. A triangular area on the western section of the dataset is markedly different from the surrounding due an issue of acquisition parameters and it cannot be merged to the rest of the dataset during the processing phase

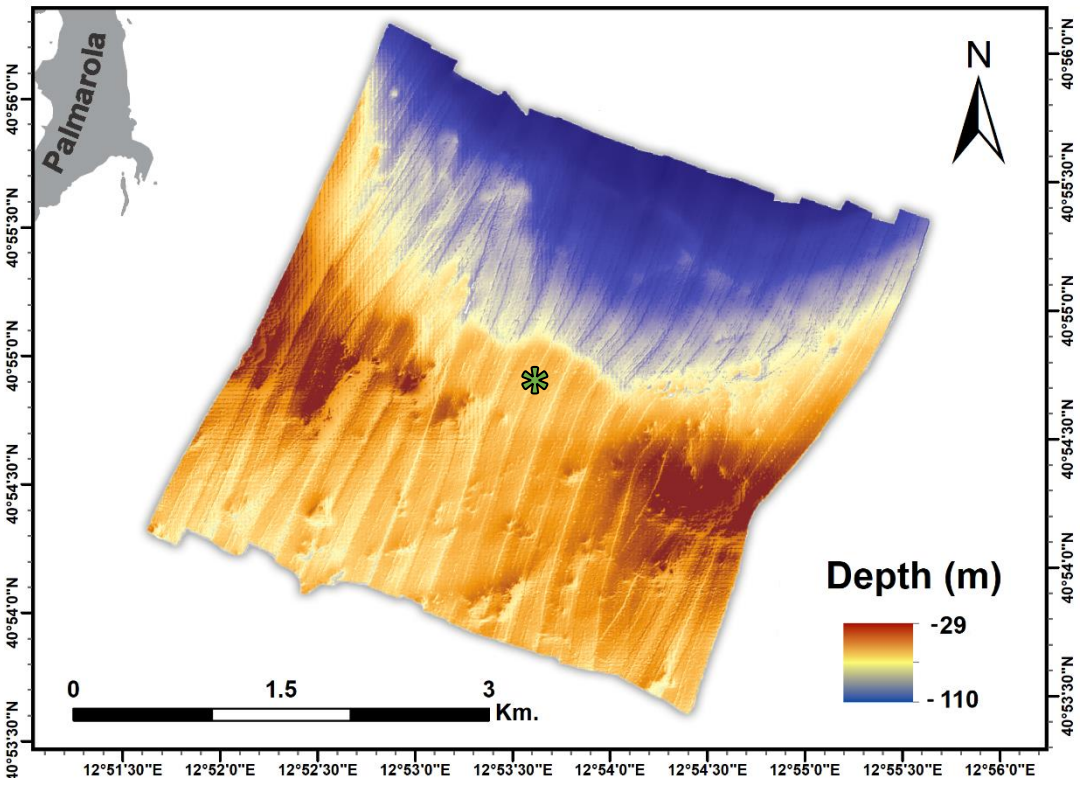

Figure 16. Map showing the general bathymetric map and features of the study area, focusing on changes in depth profile. Green star, with black outline shows the geographical centre point, as reference.

4.2. Description of the habitat

Since rhodoliths **(Fig.1)** were present, covering large parts of the visible substrate, on 67.95% (1287 from 1894) of the sample pictures, their distribution can be assessed. In this study, a rhodolith aggregation is defined and identified as a rhodolith bed, when an area of minimum 500 m^2 of sedimentary substrate has live coral coverage. Moreover, two rhodolith beds are considered distinct when their boundaries, at any given point are at least 200 m apart from each other. The extension of rhodolith habitats was estimated, considering mainly the samples' location, the RSOBIA classes and the general backscatter data. A total of three possible rhodolith beds were mapped: two at the south-western and one at the south-eastern part of the study area **(Fig.20)**. Almost all of the other ogranisms, were found on this relatively thick layer of rhodolith **(Fig.17 - A,B)**, highlighting the importance of this ecosystem and their biodiversity enhancement potential.

A total of 398 organisms were identified at least at Phylum level, from 37 distinct

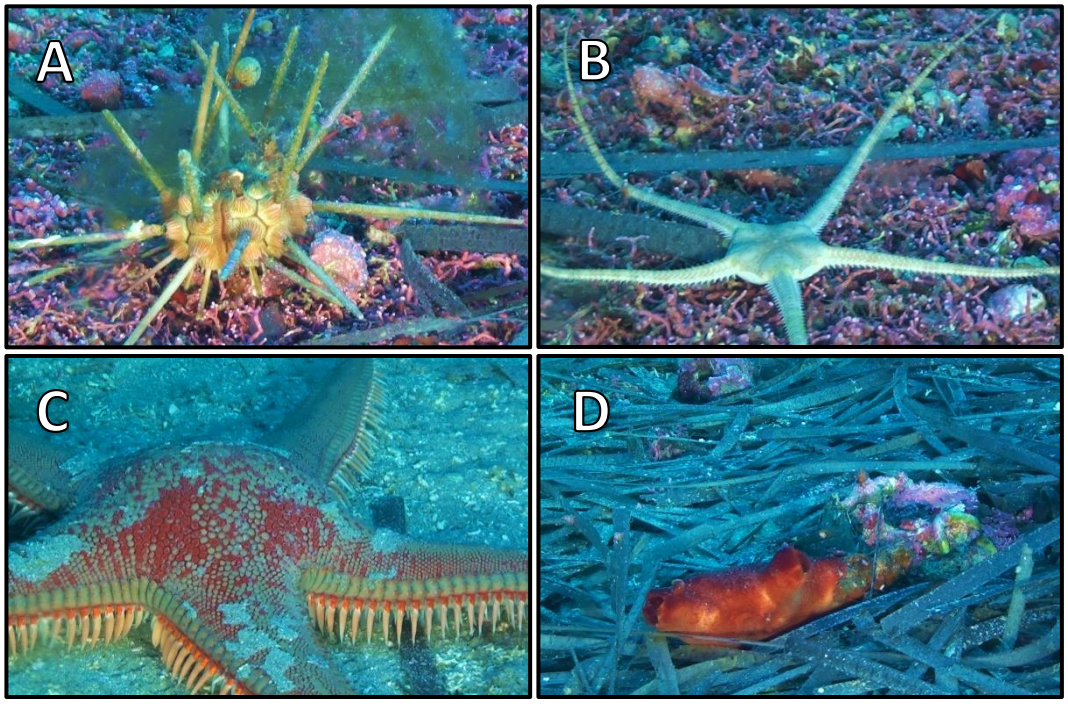

Figure 17. Subset of images from dive MS16_128, used for species identification. (A) - Cidaridae (cf. *Stylocidaris affinis*) sp.1; (B) - Ophiuroidea sp.1; (C) - *Astropecten aranciacus*; (D) – Ascidiacea sp.2

taxa **(Tab.3)**. The most abundant species across all three dives were from the cidaridae family, most likely *Stylocidaris affinis* (Philippi, 1845) **(Fig 17 - A)**. This deep-water sea urchin, also known as 'pencil urchin' occurs on circalitorral and deep sedimentary bottoms, with a wide-ranging distribution on the Mediterranean Sea. Beside their importance in maintaining the balance in benthic ecosystems, by grazing and controlling algae growth, they can be important for

science as indicator organisms for monitoring the alteration occurring at these environments (Özgür et al., 2008).

The individual organisms with the second largest number present were belonging to Phaeophyceae class. Potentially *Acinetospora crinita* ((Carmichael) Sauvageau, 1899) is the species. Beside the *A. crinita*, two more distinguishable species from the same class was documented. They were found aggregated, covering a relatively large area, mostly observed in dive MS16_21. The spread of similar assemblages, or ones with bigger sizes, mainly consisting of brown algae, can cause benthic mucilage blooms, which can threaten various habitats (Piazzi et al., 2018), by reducing the available surface for nutrient absorption of other species. Intensification of these events has been associated with global warming (Innamorati, et al. 2001) and their frequency increased also in the Mediterranean Sea.

Sporadic gorgonians, from the genus Eunicella, possibly the species of *Eunicella singularis* (Esper, 1791) was present **(Fig.18)** along the track of dive MS16_21. Temperate gorgonians are among the species most affected by climate change. Under stress conditions (mostly elevated temperature) their growth can be reduced manifold. Moreover, studies conducted on juvenile mortality and biomass reduction, showed that turf algae overgrowth **(Fig. 18 - B)** has multiple negative effects both on their recruitment and survival (Linares et al., 2012). Knowing that, many invasive Mediterranean algal species form a persistent turf, an increase in their abundance could indicate possible mass-mortality events among soft coral species.

Figure 18. Images of white gorgonians (cf. *Eunicella singularis*), observed during the video sample collection of dive MS16_21. A seemingly healthy individual (A) and one with turf algae overgrowth (B).

Among other species, ones from two distinct Sabellidae family were present at almost every dive, with 11 and 2 individuals respectively. During the dive MS16_142, the species *Myriapora truncata* (Pallas, 1766) was identified by 8 occasion, forming calcareous colonies on rocks. From the total of 1894 still images, on 222 identifiable species were present, with varying numbers. This 11.72% of visible organisms / total frames indicator is likely to be higher in reality, knowing that, if the exactly same individuals were present at multiple frames, they were only identified and counted at their first appearance, reducing the number of misleading replicates.

Using the information on the exact location of the 398 organisms identified in the area surveyed by ROV, different distribution patterns of the species/taxa can be discovered. Cidaridae family organisms are the most widespread in the area and they're distributing uniformly throughout all the sampled areas. This wide distribution of the sea urchins suggests their presence at the entire southern part of the study area. During the dive MS16_142 **(Tab. 3)** they were observed three times more in quantity, compared to other dives, highlighting an area with a relatively dense population at the south-eastern part of the study area.

While a precise benthic habitat map can't be assembled, mainly because of resolution restrictions, targeting specific organisms and their distribution can be assessed, with adequate number of observations. The resolution size of a pixel (5x5m), used in this study, is enough to detect bathymetric and acoustic reflectivity patterns related to specific features, substrates and benthic habitats, but makes the identification individual species impossible. High-quality images from ROV dives are adequate enough for finding, separating and counting the different marine organisms, a more precise taxonomical identification (e.g. at species level) can be challenging, due to external limitations. Such limitations can be the visibility, luminosity, larger distance from observed object, lack of details seen from a specific angle, etc. In these cases, the last definitive taxonomical level is chosen, to avoid the miss identification of a species.

Phylum	Class	Order	Family	Genus	Species	n° individual total	n° individual MS16_21	n° individual MS16_128	n° individual MS16_142
Annelida	Polychaeta	Sabellida	Sabellidae		sp.1	11	6	5	0
Annelida	Polychaeta	Sabellida	Sabellidae		sp.2	2	0	1	1
Arthropoda	Crustacea				sp.1	1	0	1	0
Arthropoda	Crustacea				sp.2	1	0	1	0
Arthropoda	Crustacea				sp.3	1	0	1	0
Arthropoda	Malacostraca	Decapoda	Paguridae		sp.1	1	0	1	0
Bryozoa					sp.1	4	0	0	4
Bryozoa	Gymnolaemata	Cheilostomatida	Myriaporidae	Myriapora	*Myriapora truncata* (Pallas, 1766)	8	0	0	8
Chlorophyta	Ulvophyceae	Byropsidales	Codiceae	Codium	sp.1	2	1	1	0
Chlorophyta	Ulvophyceae	Byropsidales	Codiceae	Codium	sp.2	1	1	0	0
Chlorophyta	Ulvophyceae	Cladophorales	Valoniaceae	Valonia	sp.1	1	0	0	1
Chordata	Ascidiacea				sp.1	1	1	0	0
Chordata	Ascidiacea				sp.2	1	0	1	0
Chordata	Chondrichthyes egg					1	0	1	0
Cnidaria	Anthozoa	Actineria			sp.1	4	3	1	0
Cnidaria	Anthozoa	Actineria			sp.2	2	1	0	1
Cnidaria	Anthozoa	Actineria			sp.3	3	0	0	3
Cnidaria	Anthozoa	Malacalcyonacea	Eunicellidae	Eunicella	sp.1	29	29	0	0
Echinodermata	Asteroidea				sp.1	1	0	0	1
Echinodermata	Asteroidea	Paxillosida	Astropectinidae	Astropecten	*Astropecten aranciacus* (Linnaeus, 1758)	1	0	1	0
Echinodermata	Echinoidea	Cidaroida	Cidaridae		sp.1	181	32	30	119
Echinodermata	Crinoidea				sp.1	1	0	1	0
Echinodermata	Asteroidea	Spinulosida	Echinasteridae	Echinaster	*Echinaster sepositus* (Retzius, 1805)	1	0	1	0
Echinodermata	Echinoidea				sp.1	4	0	0	4
Echinodermata	Holothuroidea				sp.1	1	0	1	0
Echinodermata	Holothuroidea				sp.2	1	0	0	1
Echinodermata	Asteroidea	Forcipulatida	Asteriidae	Marthasterias	sp.1	1	0	0	1
Echinodermata	Ophiuroidea				sp.1	3	0	3	0
Echinodermata	Echinoidea	Spatangioda	Spatangidae	Spatangus	sp.1	1	0	0	1
Mollusca	Cephalopoda	Octopoda	Octopodoidea		sp.1	1	1	0	0
Ochrophyta	Phaeophyceae				sp.1	101	98	2	1
Ochrophyta	Phaeophyceae				sp.2	19	16	2	1
Ochrophyta	Phaeophyceae				sp.3	1	0	0	1
Porifera	Demospongiae				sp.1	2	0	0	2
Rhodophyta	Florideophyceae	Corallinales			sp.1	1	1	0	0
Tracheophyta	Magnoliopsida	Alismatales			sp.1	2	0	2	0
Tracheophyta	Magnoliopsida	Alismatales			sp.2	1	0	1	0

Table 3. Taxonomical table of the identified species (at the lowest taxonomical level possible), found on the video footage of the dives MS16_21, MS16_128 and MS16_142.

4.3. RSOBIA segmentation results

The 15 detected Majority classes are showing certain patterns. 12 classes are present, occupying relatively large areas while 3 classes (0, 1, 2) are present in small patches on the Northern side of the study area. The most extensive classes are the 4th and 9th, covering around 30% of the entire map. Other major classes include the 6th and 7th, found in the middle and Southern parts. The highest differences in values were between the 5th and 14th classes, highlighting the power of backscatter intensity, used with three times weight in the segmentation.

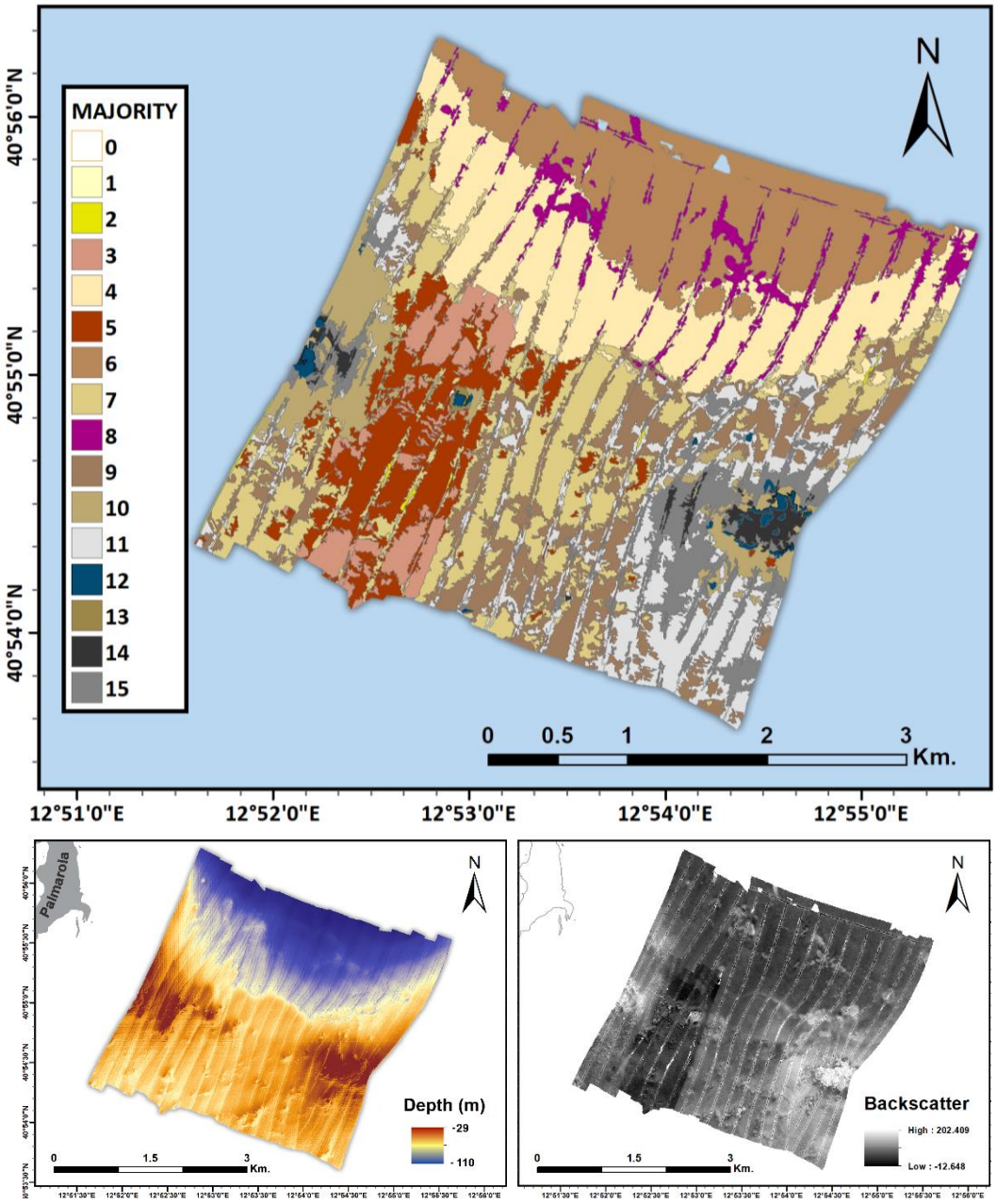

Figure 19. Results showing the 15 MAJORITY classes, created by RSOBIA segmentation. On the map, different colours indicate the spatial distribution of separate segments. Helping the comparison making, bathymetry (bottom left) and backscatter data (bottom right) is also displayed.

4.4. Benthic habitat map

Utilizing the data acquired by ROV video sampling **(3.1)** with the backscatter data, obtained with acoustic surveying **(3.3.1)**, in the classification **(3.4)** phase, five different substrate types were identified. They are present in the 15 classes created by RSOBIA segmentation **(3.3)**. Bioclastic sand (S030302) is found in 5 different classes and builds up the second largest coverage in the area. Both rock substrate (S0101) and fine unconsolidated substrate (S0303) are present in 3-3 classes respectively. Sand (S030301) is present in two neighboring classes, covering most of the seafloor in the study site. Gravelly sand (S030213) occupies 1 small class, consisting of several small patches as part of the sandy section in the North **(Fig. 19)**.

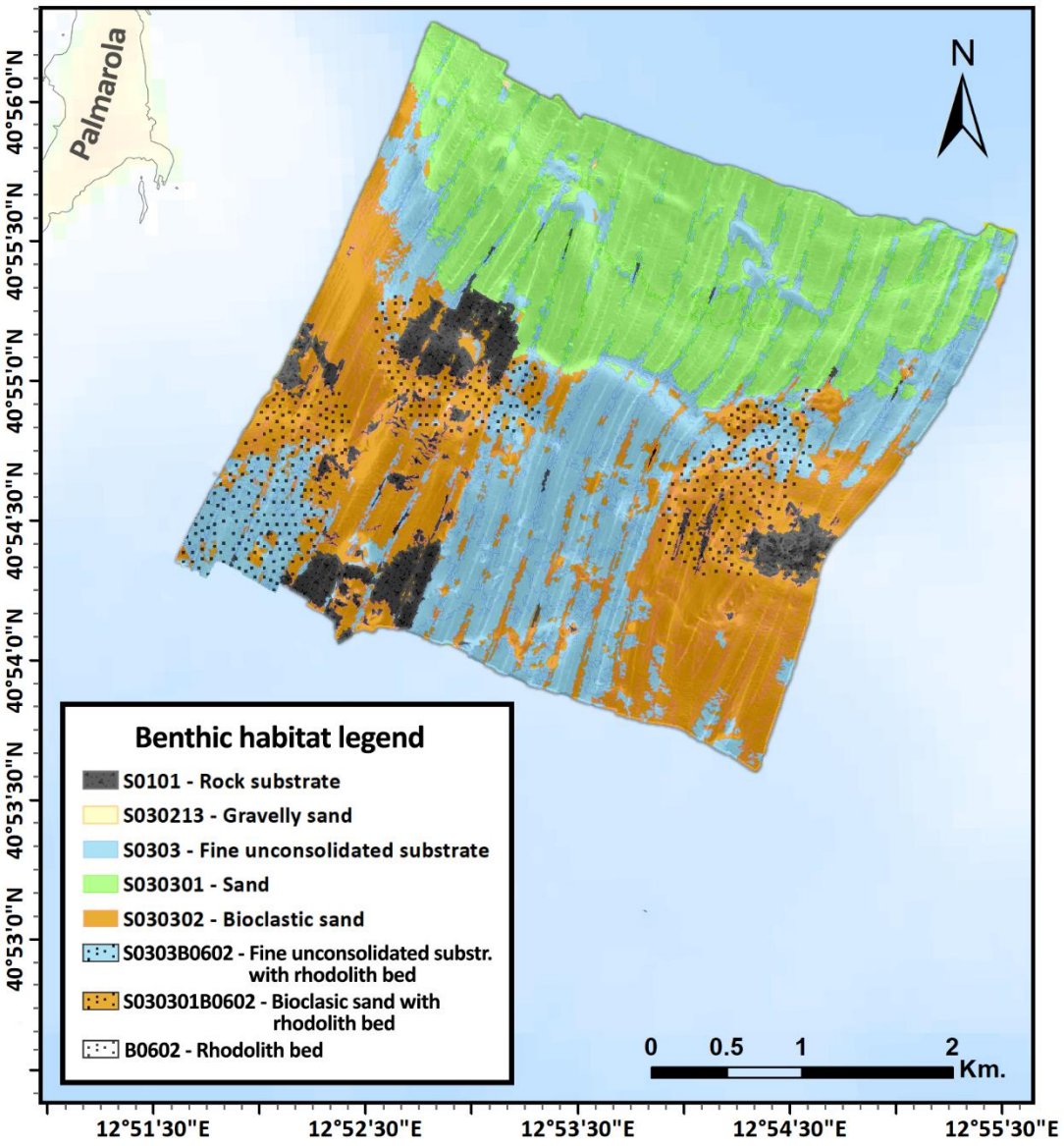

Figure 20. Benthic habitat map derived from the union of the combination of two components (substrate and biological levels) on the Pontine Islands study site. The legend reflects the CoDeMap benthic classification scheme (codes-levels).

4.5. Reliability of the model

Then, the accuracy assessment procedure here presented was run for the classes S0101 Rock substrate, S0303 Fine unconsolidated substrate, and S030302 Bioclastic sand. To predict the power and overall accuracy of these classes, a confusion matrix **(Tab.3)**, was outlined and the calculation were executed, using R statistical software.

		Reference			
		S0101	**S030302**	**S0303**	% corrected
Prediction	**S0101**	47	42	46	34.81
	S030302	10	167	79	3.91
	S0303	4	49	125	2.25
	% corrected	77.05	16.28	18.40	**59.58**

Table 3. Confusion matrix, composed by the 30% of the samples, showing how many times were they correctly predicted by the substrate map, considering also the number of occasions when they were inaccurately present in different classes (substrate type).

```
Overall Statistics

               Accuracy : 0.5958
                 95% CI : (0.5542, 0.6364)
    No Information Rate : 0.4534
    P-Value [Acc > NIR] : 6.668e-12

                  Kappa : 0.3615

 Mcnemar's Test P-Value : 2.193e-13

Statistics by Class:

                     Class: S0101 Class: S030302 Class: S0303
Sensitivity                0.7705         0.6473       0.5000
Specificity                0.8268         0.7138       0.8339
Pos Pred Value             0.3481         0.6523       0.7022
Neg Pred Value             0.9677         0.7093       0.6803
Prevalence                 0.1072         0.4534       0.4394
Detection Rate             0.0826         0.2935       0.2197
Detection Prevalence       0.2373         0.4499       0.3128
Balanced Accuracy          0.7986         0.6806       0.6669
```

Figure 21. Overall statistics, derived from results of R software, showing the model's accuracy, with significant p-value. Under the 'Statistics by Class' caption, the different Sensitivity and Specificity values are specified for each class, among other parameters.

The overall accuracy of the model is 59.58%, meaning 59.58% of the times it can predict a correct substrate type at any given location. This value is statistically significant, with the p-value < 0.01, calculated using the *caret* package in R software. The highest accuracy was observed for class S0101, with a sensitivity

value of 0.77, while the class S030302 showed a sensitivity value of 0.65. The class S0303 reported lower accuracy, with a value of 0.50.

Fine unconsolidated substrate (S0303) was the most sensitive in this comparison, but it has a specificity value of 0.83, meaning 83% of the time, the model was able to detect if in a sample which doesn't contain this substrate type, it really is not present. With other words, if a substrate categorized as not one of the three types, was really a correct no-match, or not. With almost similar value: 0.83, the rock substrate (S0101) followed, while the bioclastic sand (S030302) had a lover specificity of 0.71 **(Fig.21)**.

5. Discussion

The findings presented in this study are completely supporting the observations of Martorelli et al. 2012, concluding that bioclastic sand is one of the main substrate types, present in the area, while rhodolith beds were found to cover large proportions of the seafloor. The observations are in line with the results of the Italian Geological Mapping Project (CARG), in which a team sampled and analyzed both the seafloor sediment and marine habitats, at various locations, obtaining backscatter data, collecting grab samples and ROV images as well. The study concluded that bioclastic sand and gravel were the main sediment types, found in their locations, while coralline buildups and rhodoliths are widespread in the entirety of the study area. Mentioning that rhodoliths are the most abundant organisms, and they're forming a continuous cover on the seafloor of the Archipelago.

The study conducted by Ingrassia et al., 2014, near the Pontine Islands (NW from Palmarola and NW from Zannone Islands) used generally identical methodology and the same Urania Pollux III (GEI) ROV for the video collection samples. To locate and inspect antipatharian corals, in its study sites, used a 10x10m pixel size for its large-scale bathymetric maps, while 2x2 m pixel size for its small-scale observations. The benthic map presented in this study is bigger both in size and scale, while its 5x5 m pixel resolution is also four times higher, than the 10x10 m pixel used for covering most of the study sites, in the above mentioned one. The comparison, however is not the most convenient one, since the purposes and goals of these studies were different. Ingrassia et al., 2014 was focused on documenting coral assemblages and their distribution, while the present study, on obtaining detailed information on the substrate types and benthic habitats present in its chosen area, positioned at a different location.

A comprehensive study on the Western Pontine Archipelago, was conducted by Sañé et al., 2016, analyzing 231 grab samples and 22 hours of ROV video footage. High resolution side scan data was also obtained on a 460 km^2 area, later used for morphological classification of rhodoliths, utilizing their backscatter reflectivity. In 10% of their grab samples, live rhodoliths were present, while on 30% of ROV dives rhodoliths were observed. While the combined study area is significantly larger, compared to the present work's 15 km^2 one, the common occurrence and various morphologies, sizes and growth forms of rhodoliths show high similarity.

The limited number of substrate types obtained from the model approach used in this study, suggests a relatively homogenous substrate across the study area. From the predicted substrates only 3 were actually present in the samples, used for validation of the model. Some samples didn't provide valuable information on the substrate, mainly due image quality limitations. While rock substrate was distinct in appearance for visual identificatiom, among the other substrate types, bioclastic sand and fine unconsolidated substrate, showed visual similarity and close backscatter intensity. Dense aggregation of rhodoliths, were present in

67.95% of the samples, covering most of the upper layer of the seafloor, making the identification of the underlying substrate, which was uniformly considered as fine unconsolidated substrate challenging. In other locations, where rhodoliths weren't present, bioclastic sand dominated the sea bottom. The limitations of visibility and picture quality / resolution, allowed distinction between this type of sand and others, but the method was considered to be highly subjective, depending on the experience of the interpreter(s). Despite their close relations, limiting the predictors to just these 3 categories led to a habitat distribution model, with almost 60% accuracy. This precision can be explained with the relatively small number of referenced classes and it can be increased with the integration of more ground-truthing samples, from new locations inside the study area. Moreover, this classification of substrates and habitats is not considering many of other variables involved in their presence. Therefore, currently the distribution and borders of substrates and habitats mapped in the area, are expected to be more complex compared to how they appear.

A more recent work of Ingrassia et al. 2019, focusing on a mono-specific population of *Isidella elongata* (Esper, 1788) found in the Ventotene Basin, NW from Ventotene Island also obtained bathymetric maps on a 317 m^2, with a 3x3 m pixel resolution. While the scale and objectives were dissimilar between the studies, the methodology was almost identical, highlighting the applicability and functionality of these kind of research, supporting the mapping efforts conducted at the Pontine Islands and their surrounding area.

The method of combining multibeam echosounder data with ROV videos and grab samples, using RSOBIA, along with manual classification, offers advantages and few drawbacks. One of its strengths lies in its versatility and applicability. It can be used with various types and volumes of data, whether small or large. With the addition of semi-automated RSOBIA image segmentation, its utility extends beyond specific data types and it can be adapted for uncalibrated acoustic backscatter data as well. Moreover, this approach enables the identification of objects within images, that may not be easily distinguishable otherwise. The inclusion of ground-truth data obtained from images and samples collected from the seafloor enhances the accuracy and reliability of the analysis.

The manual classification process allows for expert oversight and modifications, ensuring the quality and precision of the results. However, this method can be time-consuming due to the fact, that the detailed and elaborated examination and alteration of the data is required. Limitations include the constraint of resolution and mapping scale, which are tied to the spatial resolution of the obtainable multi-beam data. Although the 5x5 m resolution is relatively good, it still imposes constraints on the level of details.

Furthermore, the number and spatial distribution of ground-truth data is crucial, necessitating the implication of standardized sampling methods. However, depending on the dimensions and objectives of the survey conducted, achieving a uniform sampling may be challenging.

The benthic habitat map, produced in this study increases the knowledge on the Pontine Island study site and helps completing other large-scale habitat distribution charts as well. Serves as a solid base for future monitoring activities, as an example realized in the scope of Marine Strategy Framework Directive. Although information on the precise extension of the rhodolith beds, is not enough to cover the entire study area, knowing the estimated location of these vulnerable habitats are important, both for monitoring and preserving marine ecosystems. Despite that the number of associated species to this habitat was not immense, the habitat itself is protected under 'Reefs-1170' of the Habitat Directive. Beside the geobiological purposes, gathering knowledge about this environment is crucial as supporting information for conservation measures.

6. Conclusion

The primary goals were achieved to determine the location and extension of the various habitats, focusing also on finding possible rhodolith beds, through the characterization of the seafloor.

A detailed, extensive substrate map was constructed, following a supervised methodology, with a good accuracy, therefore it can be used for versatile purposes. It includes the extension of 5 different substrate types, now categorized by the standardized CoDeMap classification scheme, which can be use in studies on sedimentation rates, sediment movements with environmental changes, anthropogenic factors on sediment quality, etc. Moreover, it can serve as useful tool, for the planning of follow-up studies, by giving valuable insights on suitable locations for data collection, monitoring, etc., in the future.

Species richness and distribution is also defined and classified by the CoDeMap classification scheme. A new habitat map, highlighting the location of three rhodolith beds was created. New information on the presence of algal turf in the area, possibly threatening other habitats, was also derived. Knowing more about the current state of the region, can also help monitoring activities, conducted in the future, by defining a baseline condition as well.

Since the acquisition of the data, used by this study was finished in 2016, further studies on the current circumstances can be conducted, highlighting the presence / absence of changes and their probable causes. By collecting samples from the same and also new locations, both the substrate type and habitat map models can be calibrated to give more accurate results. This way, tests assessing the efficiency of similar / different methods can be realized. Furthermore, relating the Pontine Islands study area, with other areas (as an example, located in different regions of the Tyrrhenian Sea or Mediterranean Sea), investigated with identical techniques, can help identify local, regional and global patterns. The obtained information can be used for decision making and can help the establishment of new MPAs.

By utilizing the capabilities of both acoustic technology and ROV imagery, the study contributes to data acquisition at a specific area, located at the Tyrrhenian Sea and to ongoing efforts, with the goal of reaching detailed information on the benthic realm and advance our understanding of these critical marine ecosystems.

7. References

Aiello, G. (2020) Bioclastic Deposits in the NW Gulf of Naples (Southern Tyrrhenian Sea, Italy): A Focus on New Sedimentological and Stratigraphic Data around the Island of Ischia. *Geochemistry*, *IntechOpen*.

Al-Wassai, F.A., Kalyankar, N.V. (2013) Major limitations of satellite images. *arXiv preprint*, 1307-2434.

Alevizos, E., Snellen, M., Simons, D., Siemens, K., Greinert, J. (2018) Multi-angle backscatter classification and sub-bottom profiling for improved seafloor characterization. *Marine Geophysics Research*, **39**, 289-306.

Amado-Filho, G.M., Bahia, R.G., Pereira-Filho, G.H., Longo, L.L. (2017) South Atlantic Rhodolith Beds: Latitudinal Distribution, Species Composition, Structure and Ecosystem Functions, Threats and Conservation Status. Rhodolith/maërl beds: a global perspective (ed. by R. Riosmena-Rodríguez, W. Nelson, W. And J. Aguirre). *Coastal Research Library, Springer, Cham*. 8-12

Ånonsen, K.B., Hagen, O.K. (2010) An analysis of real-time terrain aided navigation results from a HUGIN AUV. *OCEANS 2010 MTS/IEEE SEATTLE conference*, Seattle, WA, USA, 1-9.

Artale, V., Astraldi, M., Buffoni, G., Gasparini, G.P. (1994) Seasonal variability of gyre-scale circulation in the northern Tyrrhenian Sea. *JGR Oceans*, **99**, 14127-14137.

Ballard, R.D., McConnel, M. (1995) *Explorations: my quest for adventure and discovery under the sea.* New York: Hyperion.

Barberá, C., Bordehore, C., Borg, J.A., Glemarec, M., Grall, J., Hall-Spencer, J.M., Huz, C.D., Lanfranco, E., Lastra, M., Moore, P.G., Mora, J.A., Pita, M.E., Ramos-Esplá, A.A., Rizzo, M., Sanchez-Mata, A., Seva, A., Schembri, P.J., Valle, C. (2003) Conservation and management of northeast Atlantic and Mediterranean maerl beds. *Aquatic Conservation-marine and Freshwater Ecosystems,* **13**, 65-76.

Basso, D., Babbini, L., Kaleb., S., Bracchi, V.A., Falace, A. (2015) Monitoring deep Mediterranean rhodolith beds. *Aquatic Conservation: Marine and Freshwater Ecosystems*. **26**(3), 549–561.

Basso, D., Babbini, L., Ramos-Esplá, A. A., & Salomidi, M. (2017) Mediterranean rhodolith beds. *Rhodolith/maërl beds: A global perspective*, 281-298.

Basso, D., Bracchi, V., Caragnano, A., Caronni, S., Angeletti, L., Corselli, C. (2018) Rhodolith formation in the deep water off Marettimo, Egadi Islands, Sicily. *Abstract Book VI International Rhodolith Workshop*. *CNRS Sorbonne, Université Station Biologique de Roscoff*, 57-57.

Bianchi, C., Morri, C., Chiantore, M., Montefalcone, M., Parravicini, V., Rovere, A. (2011) Mediterranean Sea biodiversity between the legacy from the past and a future of change. *Life in the Mediterranean Sea: a look at habitat changes*, **1**, 55.

Blake, C., Maggs, C.A. (2003) Comparative growth rates and internal banding periodicity of maerl species (Corallinales, Rhodophyta) from northern Europe. *Phycologia*, **42**(6), 606–612.

Boero, F., Foglini, F., Fraschetti, S., Goriup, P., Macpherson, E., Planes, S., et al. (2016) CoCoNet: *Towards coast to coast networks of marine protected areas (From the shore to the high and deep sea), coupled with sea-based wind energy potential.* Deakin University. Journal contribution.

Brown, C.J., Blondel, P. (2009) Developments in the application of multibeam sonar backscatter for seafloor habitat mapping. *Applied Acoustics*, **70**(10), 1242-1247.

Brown, C.J., Blondel, P., Cheriton, O., Fader, G.B., & McLean, D.L. (2011) Towed camera and video sled deployments for seafloor habitat mapping in Atlantic Canada: Practical considerations, limitations, and improvements. *Canadian Journal of Fisheries and Aquatic Sciences*, **68**(1), 1-17.

Brown, C.J., Smith, S.J., Lawton, P., Anderson, J.T. (2011) Benthic habitat mapping: A review of progress towards improved understanding of the spatial ecology of the seafloor using acoustic techniques. *Estuarine, Coastal and Shelf Science*, **92**(3), 502-520.

Calder, B.R., Mayer, L.A. (2003) Automatic processing of high-rate, high-density multibeam echosounder data. *Geochemistry, Geophysics, Geosystems*, **4(**6).

Calvert, J., Strong, J.A., Service, M., McGonigle, C., Quinn, R. (2015) An evaluation of supervised and unsupervised classification techniques for marine benthic habitat mapping using multibeam echosounder data. *ICES Journal of Marine Science*, **72**(5), 1498–1513.

Chimienti, G., Angeletti, L., Rizzo, L., Tursi, A., Mastrototaro, F. (2018) ROV vs trawling approaches in the study of benthic communities: The case of *Pennatula rubra* (Cnidaria: Pennatulacea). *Journal of the Marine Biological Association of the United Kingdom*, **98**(8), 1859-1869.

Chiocci F.L., Orlando, L. (2004) Submerged depositional terraces of the Pontine Islands (Southern Latium) Mem. Descr. Carta Geol. d'It., **58**, 23-30.

Clark, M.R., Rowden, A.A., Schlacher, T.A., Williams, A., Consalvey, M., Stocks, K. I., Rogers, A.D., O'Hara, T.D., White, M., Shank, T.M, Hall-Spencer, J.M. (2010) The ecology of seamounts: Structure, function, and human impacts. *Annual Review of Marine Science*, **2**, 253-278.

Costello, M.J., Coll, M., Danovaro, R., Halpin, P., Ojaveer, H., Miloslavich, P. (2010) A census of marine biodiversity knowledge, resources, and future challenges. *PLoS ONE*, **5**(8), e12110.

Danovaro, R., Boero, F. (2019) Italian Seas, World Seas: Environmental Evaluation (Second Edition), Chapter 11, 283-306, Cambridge: Academic Press.

D'Archino, R.; Schimel, A.C.G.; Peat, C.; Anderson, T. (2021) Automated detection of large brown macroalgae using machine learning algorithms - a case study from Island Bay, Wellington. *New Zealand Aquatic Environment and Biodiversity Report*, *Ministry for Primary Industries*, **263**, 36.

Diaz, R.J., Solan, M., Valente, R.M. (2004) A review of approaches for classifying benthic habitats and evaluating habitat quality. *Journal of environmental management*, **73**(3), 165-181.

Wright, D.J., Heyman W.D. (2008) Introduction to the Special Issue: Marine and Coastal GIS for Geomorphology, Habitat Mapping, and Marine Reserves. *Marine Geodesy*, **31**(4), 223-230.

Diaz, R.J, Solan, M., Valente, R.M. (2004) A review of approaches for classifying benthic habitats and evaluating habitat quality. *Journal of Environmental Management*, **73**(3), 165-181.

Dolan M.F.J, Lucieer, V.L. (2014) Variation and Uncertainty in Bathymetric Slope Calculations Using Geographic Information Systems. *Marine Geodesy*, **37**, 187-219.

Douvere, F. (2008) The importance of marine spatial planning in advancing ecosystem-based sea use management. *Marine Policy*, **32**(5), 762-771.

Falkowski, P., Scholes, R.J., Boyle, E.E.A., Canadell, J., Canfield, D., Elser, J., Gruber, N., Hibbard, K., Högberg, P., Linder, S., Mackenzie, F.T., Moore III, B., Pedersen, T., Rosenthal, Y., Seitzinger, S., Smetacek, V., Steffen, W. (2000) The global carbon cycle: a test of our knowledge of earth as a system. *Science*, **290**(5490), 291-296.

Foglini, F., Grande, V., Marchese, F., Bracchi, V.A., Prampolini, M., Angeletti, L., Castellan, G., Chimienti, G., Hansen, I.M., Gudmundsen, M., Meroni, A.N., Mercorella, A., Vertino, A., Badalamenti, F., Corselli, C., Erdal, I., Martorelli, E., Savini, A., Taviani, M. (2019) Application of hyperspectral imaging to underwater habitat mapping, Southern Adriatic Sea. *Sensors*, **19**(10), 2261.

Foster, M.S., Steller, D.L., Riosmena-Rodríguez, R. (2015) Rhodoliths: Between rocks and soft places. *Journal of Phycology*, **51**(4), 629-641.

Halpern, B.S., Walbridge, S., Selkoe, K.A., Kappel, C.V., Micheli, F., D'Agrosa, C., John, B., Kenneth, C., Colin, E., Fujita, H., Heinemann, R., Lenihan, D., Madin, H., Perry, E., Selig, M., Spalding, E., Steneck, M., Watson, R. (2008) A global map of human impact on marine ecosystems. *Science*. **319**, 948-952.

Harris, P.T., Baker, E.K. (2012) 1 - Why Map Benthic Habitats? GeoHAB Atlas of Seafloor Geomorphic Features and Benthic Habitats, *Elsevier*, 3-22.

Henson, S.A., Sanders, R., Madsen, E. (2012). Global patterns in efficiency of particulate organic carbon export and transfer to the deep ocean. *Global Biogeochemical Cycles*, **26**(1).

Hernández-Kantún, J.J., Hall-Spencer, J.M., Grall, J., Adey, W., Rindi, F., Maggs, C.A., Bárbara, I., Peña, V. (2017) North Atlantic rhodolith beds. Rhodolith/maërl

beds: a global perspective (ed. by R. Riosmena-Rodríguez, W. Nelson and J. Aguirre). *Coastal Research Library*, *Springer, Cham.*, 265–279.

Hughes, A., Orr, M., Yang, Q., Qiao, H. (2021) Effectively and accurately mapping global biodiversity patterns for different regions and taxa. *Global Ecology and Biogeography*, **30(7)**, 1375-1388.

Hughes, C.J.E. (2018) Multibeam Echosounders. Submarine Geomorphology (ed. Micallef, A., Krastel, S., Savini, A.). *Springer Geology. Springer, Cham*., 25-41.

Iacono, R., Napolitano, E., Palma, M., Sannino, G. (2021) The Tyrrhenian Sea Circulation: A Review of Recent Work. *Sustainability*, **13**, 6371.

Ingrassia, M., Macelloni, L., Bosman, A., Chiocci, F.L., Cerrano, C., Martorelli E. (2016) Black coral (Anthozoa, Antipatharia) forest near the western Pontine Islands (Tyrrhenian Sea). *Marine Biodiversity,* **46**, 285-290.

Ingrassia, M., Martorelli, E., Bosman, A., Chiocci, F.L. (2019) *Isidella elongata* (Cnidaria: Alcyonacea): First report in the Ventotene Basin (Pontine Islands, western Mediterranean Sea). *Regional Studies in Marine Science*, **25**, 100494.

Innamorati, M., Nuccio, C., Massi, L., Mori, G., Melley, A. (2001) Mucilages and climatic changes in the Tyrrhenian Sea. *Aquatic Conservation: Marine and Freshwater Ecosystems*, **11**(4), 289-298.

Johnson, M.D., Moriarty, V.W., Carpenter, R.C. (2013) Acquiring an edge: Symbiont regulation drives host edge preference. *Science*, **340**(6137), 1584-1587.

Kostylev, V.E., Todd, B.J., Fader, G.B., Courtney, R.C., Cameron, G.D., Pickrill, R.A. (2001) Benthic habitat mapping on the Scotian Shelf based on multibeam bathymetry, surficial geology and sea floor photographs. *Marine Ecology Progress Series*, **219**, 121-137.

La Bianca, G., Rees, S., Attrill, M.J., Lombard, A.T., McQuaid, K.A., Niner, H.J., van Rein, H., Sink, K.J., Howell, K.L. (2023) A standardised ecosystem services framework for the deep sea. *Frontiers in Marine Science*, **10**(1176230).

Lanier, A., Romsos, C., Goldfinger, C. (2007) Seafloor habitat mapping on the Oregon continental margin: A spatially nested GIS approach to mapping scale, mapping methods, and accuracy quantification. *Marine Geodesy*, **30**(1-2), 51-76.

Lecours, V., Brown, C.J., Devillers, R., Lucieer, V.L., Edinger, E.N. (2016) Comparing Selections of Environmental Variables for Ecological Studies: A Focus on Terrain Attributes. *PLoS ONE*, **11**(12), e0167128.

Lecours, V., Devillers, R., Schneider, D.C., Lucieer, V.L., Brown, C.J., Edinger, E.N. (2015) Spatial scale and geographic context in benthic habitat mapping: review and future directions. Mar. Ecol. Prog. Ser., **535**, 259-284.

Lecours, V., Devillers, R., Simms, A.E., Lucieer, V.L., Brown, C.J. (2017) Towards a framework for terrain attribute selection in environmental studies. *Environmental Modelling & Software*, **89**, 19-30.

Lecours, V., Lucieer, V.L., Dolan M.F.J, Micallef, A. (2015) An Ocean of Possibilities: Applications and Challenges of Marine Geomorphometry. *Geomorphometry for Geosciences.* Adam Mickiewicz University in Poznań - Institute of Geoecology and Geoinformation, International Society for Geomorphometry, Poznań.

Levin, L.A., Sibuet, M. (2012) Understanding continental margin biodiversity: A new imperative. *Annual Review of Marine Science*, **4**, 79-112.

Linares, C., Cebrian, E., Coma, R. (2012) Effects of turf algae on recruitment and juvenile survival of gorgonian corals. *Mar. Ecol. Prog. Ser.*, **452**, 81-88.

Lindner, G., Cairns, S.D., Cunningham, C.W. (2008) From offshore to onshore: multiple origins of shallow-water corals from deep-sea ancestors. *PLoS ONE*, **3(6)**, e2429.

Linley, T.D., Gerringer, M.E, Yancey, P.H., Drazen, J.C., Weinstock, C.L., Jamieson, A.J. (2016) Fishes of the hadal zone including new species, in situ observations and depth records of Liparidae. Deep Sea Research Part I: *Oceanographic Research Papers*, 114, 99-110.

Lim, A., Huvenne, V.A., Vertino, A., Spezzaferri, S., Wheeler, A.J. (2018) New insights on coral mound development from groundtruthed high-resolution ROV-mounted multibeam imaging. *Marine Geology*, **403**, 225-237.

Long, R. (2015) The Marine Strategy Framework Directive: A New European Approach to the Regulation of the Marine Environment, Marine Natural Resources and Marine Ecological Services. *Journal of Energy & Natural Resources Law*, **28**, 1-44.

Lucieer, V., Hill, N.A., Barrett, N.S., Nichol, S. (2013) Do marine substrates 'look' and 'sound' the same? Supervised classification of multibeam acoustic data using autonomous underwater vehicle images. *Estuarine Coastal and Shelf Science*, **117**, 94–106.

Lucieer, V., Hill, N.A., Barrett, N.S., Nichol, S. (2017). Do marine substrates 'look' and 'sound' the same? Supervised classification of multibeam acoustic data using autonomous underwater vehicle images. *Estuarine, Coastal and Shelf Science*, **198**, 139-147.

Lurton, X. (2002) An introduction to underwater acoustics: *principles and applications.* Bodmin, Cornwall: MPG Books Ltd.

Lutz, M.J., Caldeira, K., Dunbar, R.B., Behrenfeld, M.J. (2007) Seasonal rhythms of net primary production and particulate organic carbon flux to depth describe the efficiency of biological pump in the global ocean. *Journal of Geophysical Research: Oceans*, **112**(C10).

Macreadie, P.I., McLean, D.L., Thomson, P.G., Partridge, J.C., Jones, D.O.B., Gates, A.R., Benfield, M.C., Collin, S.P., Booth, D.J., Smith, L.L., Techera, E., Skropeta, D., Horton, T., Pattiaratchi, C., Bond, T., Fowler, A.M. (2018) Eyes in the sea: Unlocking

the mysteries of the ocean using industrial, remotely operated vehicles (ROVs), *Science of The Total Environment*, **634**, 1077-1091.

Martorelli, E., D'Angelo, S., Fiorentino, A., Chiocci, F.L. (2012) 31 - Nontropical Carbonate Shelf Sedimentation. The Archipelago Pontino (Central Italy) Case History. *GeoHAB Atlas of Seafloor Geomorphic Features and Benthic Habitats*, 449-456.

Mastrototaro, F., Montesanto, F., Tursi, A., Aguilar, R., Chimienti, G. (2021) Biometry supporting species identification from underwater images in two Mediterranean Sea urchins. *2021 International Workshop on Metrology for the Sea; Learning to Measure Sea Health Parameters (MetroSea)*, 91-94.

Mayer, L., Jakobsson, M., Allen, G., Dorschel, B., Falconer, R., Ferrini, V., ..., Weatherall, P. (2018). The Nippon Foundation—GEBCO seabed 2030 project: The quest to see the world's oceans completely mapped by 2030. *Geoscience Letters*, **5**(1), 1-8.

McFarlane, J.R. (2000) Underwater technology 2000 ROVs and AUVs: tools for exploring, exploiting and defending the ocean frontier. *Proceedings of the 2000 International Symposium on Underwater Technology, Tokyo*, 465-471.

McLean, D.L., Parsons, M.J.G., Gates, A.R., Benfield, M.C., Bond, T., Booth, D.J., Bunce, M., Fowler, A.M., Harvey, E.S., Macreadie, P.I., Pattiaratchi, C.B., Rouse, S., Partridge, J.C., Thomson, P.G., Todd, V.L.G., Jones, D.O.B. (2020) Enhancing the Scientific Value of Industry Remotely Operated Vehicles (ROVs) in Our Oceans. *Frontiers in Marine Science*, **7**.

Millot, C. (1999) Circulation in the Western Mediterranean Sea. Journal of Marine Systems, **20**, 423-442.

Misiuk, B., Brown, C.J. (2024) Benthic habitat mapping: A review of three decades of mapping biological patterns on the seafloor. *Estuarine, Coastal and Shelf Science*, **296**, 108599.

Mitchell, A.J., Flanagan, C., Strong, J.A., Service, M., 2007. The Application of Optimal Allocation Analysis to the Stratification of Ground-Truth Sampling in Benthic Habitat Mapping. MESH Project Guidance Document Worked Example.

Niz, W.C., Laurino, I.R.A, de Freitas, D.M., Rolim, F.A., Motta, F.S., Pereira-Filho, G.H. (2023) Modeling risks in marine protected areas: Mapping of habitats, biodiversity, and cultural ecosystem services in the southernmost atlantic coral reef. *Journal of Environmental Management*, **345**, 118855.

Palmiotto, C., Loreto, M.F. (2019) Regional scale morphological pattern of the Tyrrhenian Sea: New insights from EMODnet bathymetry. *Geomorphology*, **332**, 88-99.

Piazzi, L., Atzori, F., Cadoni, N., Cinti, M. F., Frau, F., Ceccherelli, G. (2018) Benthic mucilage blooms threaten coralligenous reefs. *Marine environmental research*, **140**, 145-151.

Pickrill, R.A., Kostylev, V.E. (2007) Habitat mapping and national seafloor mapping strategies in Canada. *Mapping the Seafloor for Habitat Characterization:* Geological Association of Canada, **47**, 483-495.

Prampolini, M., Angeletti, L., Castellan, G., Grande, V., Le Bas, T., Taviani, M., Foglini, F. (2021) Benthic Habitat Map of the Southern Adriatic Sea (Mediterranean Sea) from Object-Based Image Analysis of Multi-Source Acoustic Backscatter Data. *Remote Sens*, **13**, 2913

Raimondi, S. (2014) Natural values, coastal and marine ecosystems of the Circeo National Park: conservation priorities. Biodiversity Journal, **5**(2), 147-150.

Rebelo, A.C., Johnson, M.E, Rasser, M.W., Silva, L., Melo, C.S., Ávila, S.P. (2021) Global biodiversity and biogeography of rhodolith-forming species. *Frontiers of Biogeography*, **13**(1), e50646.

Rendina, F., Buonocore, E., Cocozza di Montanara, A., Russo, G.F. (2022) The scientific research on rhodolith beds: A review through bibliometric network analysis. *Ecological Informatics*, **70**, 1574-9541.

Rendina, F., Kaleb, S., Caragnano, A., Ferrigno, F., Appolloni, L., Donnarumma, L., Russo, G.F., Sandulli, R., Roviello, V., Falace, A. (2020) Distribution and Characterization of Deep Rhodolith Beds off the Campania coast (SW Italy, Mediterranean Sea). *Plants*, **9**, 985.

Riley, S. J., DeGloria, S. D., Elliot, R. (1999) A terrain ruggedness index that quantifies topographic heterogeneity. *Intermountain Journal of Sciences*, **5**, 23-27.

Riosmena-Rodríguez, R. (2017) Natural history of rhodolith/maërl beds: their role in near-shore biodiversity and management. Rhodolith/maërl beds: a global perspective (ed. by R. Riosmena-Rodríguez, W. Nelson, W. And J. Aguirre). *Coastal Research Library, Springer, Cham.,* 3-26*.*

Ritondale, M. (2014) Deep discoveries from the seabed of the Pontine Islands: the shipwrecks of Ventotene, Santo Stefano and Zannone. *Assemblage*, **13**, 26-38.

Rösler, A., Perfectti, F., Peña, V., Braga, J.C. (2016) Phylogenetic relationships of corallinaceae (Corallinales, Rhodophyta): taxonomic implications for reef-building corallines. *Journal of Phycology*, **52**, 412–431.

Sañé, E., Chiocci, F. L., Basso, D., Martorelli, E. (2016). Environmental factors controlling the distribution of rhodoliths: An integrated study based on seafloor sampling, ROV and side scan sonar data, offshore the W-Pontine Archipelago. *Continental Shelf Research*, **129**, 10-22.

Schimel, A.C.G., Healy, T.R., Johnson, D., Immenga, D. (2010) Quantitative experimental comparison of single-beam, sidescan, and multibeam benthic habitat maps. *ICES Journal of Marine Science*, **67**(8), 1766–1779.

Steller, D. L., Riosmena-Rodríguez, R., Foster, M. S. (2016). Rhodolith bed diversity in the Gulf of California: The importance of rhodolith structure and consequences

of disturbance. Aquatic Conservation: Marine and Freshwater Ecosystems, 26(5), 901-918.

Strong, J.A., Clements, A., Lillis, H., Galparsoro, I., Bildstein, T., Pesch, R. (2019) A review of the influence of marine habitat classification schemes on mapping studies: inherent assumptions, influence on end products, and suggestions for future developments. *ICES Journal of Marine Science*, **76**(1), 10-22.

Talkington, H. (1983) History And Accomplishments In Ocean Engineering At The Naval Ocean Systems Center, 1966-1983. *Proceedings OCEANS 1983,* 384-387.

Le Bas, T. (2016) RSOBIA – A new OBIA Toolbar and Toolbox in ArcMap 10.x for Segmentation and Classification. GEOBIA 2016: Solutions and Synergies Conference.

Özgür, E., Öztürk, B., Karakulak, S. (2008) The Echinoderm Fauna of Turkey with new records from the Levantine coast of Turkey. *The 2nd Scientific Conference of Animal Wealth Research in the Middle East & North Africa*, **16**, 18.

Ventura, G., Milano, G., Passaro, S., Sprovieri, M. (2013) The Marsili Ridge (Southern Tyrrhenian Sea, Italy): An island-arc volcanic complex emplaced on a 'relict' back-arc basin. Earth-Science Reviews, **116**, 85-94.

Verfaillie, E., Doornenbal, P., Mitchell, A.J., White, J. and Van Lancker, V. (2007) The bathymetric position index (BPI) as a support tool for habitat mapping. Worked example for the MESH Final Guidance, 14 pp.

Walbridge, S., Slocum, N., Pobuda, M., Wright, D.J. (2018) Unified Geomorphological Analysis Workflows with Benthic Terrain Modeler. *Geosciences*, **8**, 94.

Warren, S.D., Hohmann, M.G., Auerswald, K., Mitasova, H. (2004) An evaluation of methods to determine slope using digital elevation data. *CATENA*, **58**(3), 215-233.

Watling, L., Guinotte, J., Clark, M. R., & Smith, C. R. (2013). A proposed biogeography of the deep ocean floor*. Progress in Oceanography*, **111**, 91-112.

Weiss, A.D. (2001) Topographic positions and landforms analysis. ESRI International User Conference, San Diego, California.

Wilson, M.F., O'Connel, B., Brown, C., Guinan, J.C., Grehan, A. (2007) Multiscale Terrain Analysis of Multibeam Bathymetry Data for Habitat Mapping on the Continental Slope. *Marine Geodesy*, **30**, 3-35.

Wölfl, A.C., Snaith, H., Amirebrahimi, S., Devey, C.W., Dorschel, B., Ferrini, V., Huevenne, V.A.I, Jakobsson, M., Jencks, J., Jhonston, G., Lamarche, G., Mayer, L., Millar, D., Pedersen, T.H., Picard, K., Reitz, A., Schmitt, T., Visbeck, M., Weatherall, P., Wigley, R. (2019) Seafloor mapping–the challenge of a truly global ocean bathymetry. *Frontiers in Marine Science*, 283.

Wozencraft, J., Millar, D. (2005) Airborne lidar and integrated technologies for coastal mapping and nautical charting. *Marine Technology Society Journal*, **39**(3), 27-35.

Wynn, R.B., Huvenne, V.A.I., Le Bas, T.P., Murton, B.J., Connelly, D.P., Bett, B.J., Ruhl, H.A., Morris, K.J., Peakall, J., Parsons, D.R., Sumner, E.J, Darby, S.E., Dorrell, R.M., Hunt, J.E. (2014) Autonomous Underwater Vehicles (AUVs): Their past, present and future contributions to the advancement of marine geoscience. *Marine Geology*, **352**, 451-468.

Yesson, C., Taylor, M. L., Tittensor, D. P., Davies, A. J., Guinotte, J., Baco, A., Black, J., Hall-Spencer, J.M, Rogers, A.D. (2012) Global habitat suitability of cold-water octocorals. *Journal of Biogeography*, **39(7)**, 1278-1292.

Yuh, J., West, M. (2001) Underwater robotics. *Advanced Robotics*, **15**(5), 609-639.

8. Supplementary Information

Segmentation	Terrain Attributes	Weight	Nr. Of Clusters	Min. Object size	Result Usefullness
1	Backscatter	1	8	50	Low
	BPI	1			
	Bathymetry	1			
	Slope	1			
	Rugeddness	1			
2	Backscatter	2	8	50	Low
	BPI	2			
	Bathymetry	1			
	Slope	1			
	Rugeddness	1			
3	Backscatter	3	8	50	Low
	BPI	2			
	Bathymetry	1			
	Slope	1			
	Rugeddness	1			
4	Backscatter	2	15	50	Medium
	BPI	2			
	Bathymetry	1			
	Slope	1			
	Rugeddness	1			
5	Backscatter	3	15	50	Medium
	BPI	2			
	Bathymetry	1			
	Slope	1			
	Rugeddness	1			
6	Backscatter	3	15	50	High
	BPI	1			
	Bathymetry	1			
	Slope	1			
	Rugeddness	1			

Table 4. Portion of a larger table, used to test and find the adequate weight for the terrain attributes, used in the segmentation, combined with the previously fixed minimum object size and the varying number of clusters parameters. After the most suitable numbers are decided for one parameter, the others can be altered accordingly. This study doesn't include a perfect solution for this process, it's mostly depending on the expert's interpretation. By running the RSOBIA segmentation algorithm multiple times, with altered parameters, the results can be related to each other, to find the most suitable polygon classification. In this example, initially 8 clusters were tested, giving different weights to the already fixed terrain attributes, giving insufficient results. Later, keeping the different weights, the number of clusters were increased, giving better and better results, reaching the one, which is used in the study (6th segmentation).

5 clusters (50 min. obj. Size)		
Value	Label	Count
0	0	3
1	1	11
2	2	82
3	3	13
4	4	169
5	5	56
5 clust.	**total**	**334**
	avg/clust.	**55.67**
	avg/total	**0.17**

10 clusters (50 min. obj. Size)		
Value	Label	Count
0	0	4
1	1	8
2	2	38
3	3	49
4	4	14
5	5	178
6	6	232
7	7	139
8	8	141
9	9	14
10	10	40
10 clust.	**total**	**857**
	avg/clust.	**77.91**
	avg/total	**0.09**

15 clusters (50 min. obj. Size)		
Value	Label	Count
0	0	5
1	1	3
2	2	7
3	3	49
4	4	39
5	5	76
6	6	12
7	7	193
8	8	120
9	9	235
10	10	52
11	11	238
12	12	25
13	13	3
14	14	20
15	15	119
15 clust.	**total**	**1196**
	avg/clust.	**74.75**
	avg/total	**0.06**

20 clusters (50 min. obj. Size)		
Value	Label	Count
0	0	3
1	1	5
2	2	9
3	3	80
4	4	54
5	5	45
6	6	90
7	7	54
8	8	174
9	9	151
10	10	87
11	11	235
12	12	1
13	13	201
14	14	64
15	15	64
16	16	19
17	17	52
18	18	18
19	19	90
20	20	2
20 clust.	**total**	**1498**
	avg/clust.	**71.33**
	avg/total	**0.05**

25 clusters (50 min. obj. Size)		
Value	Label	Count
0	0	170
1	1	217
2	2	31
3	3	23
4	4	768
5	5	440
6	6	819
7	7	1136
8	8	999
9	9	1411
10	10	1862
11	11	2021
12	12	444
13	13	795
14	14	2637
15	**15**	0
16	16	2443
17	17	530
18	18	534
19	19	23
20	20	78
21	21	10
22	22	83
23	23	484
24	24	1608
25	25	984
25 clust.	**total**	**20550**
	avg/clust.	**790.38**
	avg/total	**0.04**

Figure 22. Small tables, used to find the most suitable number of clusters for this study. The minimum object size is fixed to 50 in every occasion. The number of clusters start from 5, and each time they're increased by 5, reaching 25 at the final segmentation. From the 5 - test segmentation, the MAJORITY attribute is examined, showing how many polygons are used and classified inside a specific cluster. As an example, looking at the MAJORITY values of the 5 - cluster segmentation (grey table) a total of 334 polygons were classified and collected inside the clusters: 11 being in the first cluster, 82 in the second and so on. The average number of polygons inside one cluster is 55.67. Moving towards the segmentation with 25 clusters, we see an increase in the number of total polygons used (which indicates positive direction, meaning the classification will capture more bathymetric details) and the average number of polygons/cluster. At the 20 - cluster segmentation (blue table) this value starts to shrink, indicating an adequate enough cluster number (the algorithm is not able to put more polygons to specific cluster), while at the 25 - cluster segmentation (orange table) we observe the first empty cluster (red cells) indicating the maximum cluster size is reached (after which empty classes start to appear). The overall trend indicates, that the number of clusters capturing the most of the data, without significant drawback, is around 20 clusters. The 15 - cluster segmentation (green table) was used, because of the overall distribution of polygons in each cluster.